Water Resources Research Institute
of The University of North Carolina

Report No. 441

OPTIMIZING SOIL-POLYACRYLAMIDE INTERACTIONS FOR EROSION CONTROL AT CONSTRUCTION SITES

By
Richard McLaughlin, Aziz Amoozegar, Owen Duckworth, Joshua Heitman

Soil Science Department
North Carolina State University
Raleigh, NC

UNC-WRRI-441

The research on which this report is based was supported by funds provided by the North Carolina General Assembly and/or the US Geological Survey through the NC Water Resources Research Institute.

This report fulfills the requirements for a project completion report of the Water Resources Research Institute of The University of North Carolina. The authors are solely responsible for the content and completeness of the report.

WRRI Project No. 12-06-W
January 2014

Optimizing Soil-Polyacrylamide Interactions for Erosion Control at Construction Sites

ABSTRACT

Regulations on construction site runoff are tightening and will likely lead to adoption of improved erosion control practices, including the application of polyacrylamide (PAM) to soil to enhance erosion and sediment control. While the benefits of PAM applications in reducing erosion have been well demonstrated for agricultural applications, it is not clear how the applied PAM differing in formations interact with soil material and how much of the applied PAM can be lost, impacting the end result for the construction site application. The project was initiated to investigate the soil-PAM interactions to obtain the maximum benefits from the PAM applied for erosion and sediment control. The project was conducted in three phases: 1) method development for quantifying dissolved PAM, 2) rainfall simulation study, and 3) laboratory column and sorption experiments. In the first phase, we developed a modified turbidimetric method using cationic surfactant (hyamine 1622) and it was proven to be a quick and reliable method for quantifying PAM in soil extracts at low carbon content. In the second phase, a rainfall simulation study was conducted to evaluate the performance of an excelsior erosion control blanket (cover) and two PAM application methods (dissolved vs granule). Runoff turbidity and total suspended solids (TSS) from PAM treatments with cover were at least 28-times less than those of control (2315 nephelometric turbidity units, 2777 mg TSS L^{-1}), with the cover + dissolved PAM being the most effective in delaying runoff initiation and reducing TSS. As a result of flocculation, eroded sediments collected from PAM treatments had 7- to 9-times greater median particle diameter than those from the control (12.4 µm). Loss of PAM for the granular PAM treatment was 19% of applied PAM, but was only 2% of applied PAM for the dissolved PAM treatment. While both PAM formulations applied with a temporary groundcover were effective in improving runoff water quality, applying dissolved form resulted in greater benefits with a lower PAM loss. In the third phase, we investigated dissolved PAM penetration in 2-cm thick sandy clay loam soils under saturated condition in two application modes (pulse and continuous). The pulse input of dissolved PAM applied at the typical hydroseeding rate (30 kg ha^{-1} in 500 mg PAM L^{-1}) decreased the hydraulic conductivity (HC) by a 100-fold and allowed 14 % of the applied PAM to leached out. Continuously applied 25 mg L^{-1} of dissolved PAM solution decreased the HC by a 10,000-fold and leached PAM only accounted for 23 % of the total amount of applied PAM with given 130 pore volume of PAM throughput, demonstrating strong retardation of the dissolved PAM within the 2-cm soil layer. The PAM transport simulation by the CXTFIT was best described with a dual-porosity model (mobile and immobile), suggesting that the viscous PAM solution used in our study established physical non-equilibrium condition in the soil columns. Under typical conditions, it does not appear significant amounts of PAM applied for erosion control will wash away or leach very far into the soil.

TABLE OF CONTENTS

LIST OF TABLES

LIST OF FIGURES

ACKNOWLEDGMENTS

We gratefully thank the NC Water Resources Research Institute which funded this project. Most of the data collection, analyses, and report preparation were conducted by postdoctoral research scholar Dr. Jihoon Kang, research technician Jamie Luther, and extension associate, Jacob Wiseman. We like to thank you to two undergraduate students, Tyler Sowers and McKhenzy Welch for their assistance in lab and field work.

1. Introduction and Study Objectives

1.1. Statement of the Regional Water Problems

The NC population is estimated to increase to 9.3 million by 2025 (Bureau of Census, 2010), and a massive amount of construction will be required to provide housing and infrastructure for the expanding population. Rapid growth is expected for many population centers in North Carolina that are in close proximity to water supply reservoirs or other important water resources. Under the current practices, areas considered for large developments and highway construction sites are completely cleared, exposing subsoils that pose a severe erosion risk. Construction sites are generally prone to high erosion rates because they cover large areas, are highly disturbed, have no cover for an extended period of time, and are often on steep slopes. Despite US Environmental Protection Agency (EPA) guidelines and state regulations concerning erosion from construction activities, construction sites are subject to significant amount of erosion during rainfall events that produce runoff. It is estimated that sediment loads from construction projects can be 2,000 times greater than wooded areas and 10 to 20 times greater than agricultural fields (Novotny and Olem, 1994). Erosion from construction sites may exceed 10 metric tons soil/ha for a single rainfall event (Hayes et al., 2005). In addition to reducing reservoir capacity, soil erosion resulting in the transport of soil particles by storm water runoff is considered the most widespread cause of pollution of streams and lakes (USEPA, 2002). Thus, controlling erosion on construction sites is critical to the protection of water resources in North Carolina.

According to Moreau (1992), from the 1970s to early 1990s, North Carolina experienced no expansion of public water supply reservoirs, and even saw a decline in recreational reservoirs. Therefore, the impact of sediment loading from construction sites on water supply reservoirs poses a serious threat to ecosystem health and the public supply of safe drinking water. McLaughlin et al. (2009) indicates streams adjacent to construction sites may be more heavily impacted with sediment loading during storm events than previously reported (Erhart et al. 2002). To highlight the impact of potential surface water pollution by erosion, consider that Chatham and Durham Counties, which contain most of the Jordan Lake shoreline, increased the number of housing units 23% from 2000 to 2008 (Southern Rural Development Center, 2010). Because these subdivisions will most likely be sited within 40 km of the lake, sediments released during construction of these developments will be deposited in Jordan Lake. Similar growth is expected for many other counties, such as Alamance, Orange, and Wake, most of which drain to Jordan Lake, Falls Lake, or another water supply reservoir.

The most common practice for reducing release of soil particles to streams and lakes is the use of ponding devices to trap sediment through settling. The amount of soil transported by erosion that can settle in a sediment trap depends on the particle size distribution of the soil subjected to erosion. According to Line and White (2001), a typical sediment trap can only retain 50 to 60% of the sediments that enter it. A simple calculation using Stokes law (Hillel, 2004) shows that while it takes just under 6 minutes for all sand-sized particles (>0.05 mm in diameter) to settle to the bottom of a 1 m deep sediment trap, it takes more than 61 hours for all silt-sized particles (> 2 μm) to settle to that depth, and it takes more than 2 days for clay-sized particles larger than 1 μm to settle through the upper 20 cm of the suspension in the sediment trap (> 10 days to settle 1 m). Recent regulation issued by USEPA (2009), entitled the Effluent Limit Guidelines (ELG), mandates that the turbidity of water released from construction sites not to exceed 280 nephelometric turbidity units (NTU). While the specific turbidity target is now under further

review (US EPA, 2011), this regulation will likely require the implementation of new erosion control approaches (both physical and chemical) and/or some form of on-site treatment of runoff to address turbidity.

1.2. Polyacrylamide for Erosion and Turbidity Control

Minimizing the impact of current construction practice on nearby surface waters requires continued development of innovative erosion control practices. The use of polyacrylamide (PAM) has gained wide acceptance for reducing soil erosion and improving runoff water quality in agricultural fields and construction sites. The primary functions of PAM application are two-fold: 1) a flocculating agent for suspended materials in aqueous suspension and 2) an aggregating agent for soil conditioning. Application of PAM for land management has proven to be effective and economical in stabilizing soil structure, reducing soil erosion, and improving runoff water quality (Hayes et al., 2005; Sojka et al., 2007; Kang et al. 2013b). As its use has become more widespread, determination of PAM concentration in soil water (e.g., runoff water, groundwater, soil solution) has also become increasingly important to better understand the fate and transport of PAM in the environment (Lu and Wu, 2003a).

Polyacrylamide is a broad class of synthetic organic polymers formed by the polymerization of acrylamide (AMD) units and it can be synthesized to have specific chemical properties, including net charge (anionic, neutral, or cationic), charge density (% hydrolysis), and molecular weight. Cationic PAMs are usually avoided in environmental applications due to their potential aquatic toxicity (Barvenik, 1994). High-molecular weight, linear, anionic PAMs are used for soil and water conservation purposes as they adsorb to soil irreversibly through linkages between the anionic groups and the negatively charged soil constituents by exchangeable cation bridges (Seybold, 1994). Whereas PAM is stable and non-toxic, the residual AMD monomers raise concerns as a neurotoxin and a skin irritant (Rudén, 2004). Commercial grade PAMs for water treatment have <0.05 % AMD monomer, which is considered to be a safe level when used at low concentration (Barvenik, 1994; Sojka et al., 2007). Nonetheless, potential concerns highlight need for reliable analytical methods for the quantification of PAM in environmental samples.

Lu and Wu (2003a) reviewed the existing analytical methods for quantifying aqueous PAM concentration. They emphasized that any method for quantifying PAM in soil waters should be sensitive at low concentrations (< 1 mg L^{-1}) and insensitive to interferences such as dissolved salts and organic matter (OM). The analytical methods for aqueous PAM are generally based on 1) the chemical properties of amide groups in PAM assessed by N-bromination of the amides (Scoggins and Miller, 1979; Lu and Wu, 2001); 2) the physical properties of the PAM solution determined by viscosity measurement (Jungreis, 1981), flocculation-based methods (Lentz et al., 1996), or size exclusion chromatography (Hunt et al., 1988); 3) the combined physical and chemical properties determined by turbidimetric methods (Allison et al., 1987) or polarography (Smith-Palmer et al., 1988); and 4) methods based on total organic carbon (TOC) concentration and radioactive labeling (Ben-hur et al., 1992; Entry et al., 2008). Most of these methods are complicated procedures that may require expensive laboratory equipment. The TOC measurement is considered to be the simplest method, but it is not selective for PAM as the analytical signal responds to all dissolved organic substances (Lu and Wu, 2003a). An alternate and equally simple analytical procedure based on turbidimetry may provide an improved method

to quantify PAM in solution with higher selectivity, if the interferences from salts and OM are minimal (Taylor and Nasr-El-Din, 1994).

The turbidimetric method for quantifying PAM uses a reagent that reacts with AMD subunits in anionic PAMs to produce insoluble colloids that remain suspended in solution, giving rise to turbidity. Hyamine 1622 (benzethonium chloride; referred to as "Hyamine") is the most commonly used turbidimetric reagent for anionic PAMs (Michaels and Morelos, 1955; Crummett and Hummel, 1963; Wimberley and Jordan, 1971; Allison et al., 1987). When a large anionic polyelectrolyte reacts with a large cationic molecule such as hyamine, optical density determined by a turbidimeter or a spectrophotometer is proportional to the concentration of PAM in solution. Previous studies determined that the methods based on hyamine had detection limits of 0.5 to 1 mg L^{-1} for dissolved PAM in either deionized (DI) water or oil-field brines (Crummett and Hummel, 1963; Allison et al., 1987; Taylor and Nasr-El-Din, 1994). These results suggest that the hyamine test may be useful for quantifying PAM in environmental soil water samples.

The efficacy of PAM in reducing erosion from irrigated agricultural fields has been well established (Aase et al., 1998; Lenz and Sojka, 2009; Sojka et al., 1998), as well as its impact on hydraulic conductivity and intake rate of field soils and depositional seals (Bhardwaj et al., 2009; 2010; Helalia and Levy, 1988; Sirjacob et al., 2000). However, fewer studies have addressed the use of PAM on the steep, highly compacted slopes typical of construction sites (Sojka et al., 2007). While it is clear that PAM can greatly reduce erosion and improve runoff water quality, there is little information on how to optimize the application for the greatest effect under these challenging conditions. Hayes et al. (2005) and Soupir et al. (2004) found that application of PAM on bare surfaces at construction sites at recommended rate of 10.5 kg/ha or less did not effectively control sediment transport or reduce turbidity of runoff water. Flanagan et al. (2002a, 2002b) found that a much higher rate (80 kg/ha) and concentration significantly reduced erosion on bare, steep slopes, but they were testing it on slopes with well-tilled topsoil. Compared to PAM alone, mulches are much more effective in protecting slopes from erosion (Soupir et al., 2004; Hayes et al., 2005) and PAM can enhance that protection (McLaughlin and Brown, 2006; Babcock and McLaughlin, 2011).

Sojka et al. (2007) suggested that the high concentrations used in typical hydroseeding operations, as evaluated by Soupir et al. (2004) and Hayes et al. (2005), may have contributed to poorer erosion control by PAM. They further suggested that for PAM to be effective at high concentrations (up to 468 mg/L), the soil would need to be completely dry before application, or that higher volumes of water would be needed to adequately transport PAM to deeper depths in the soil. However, Flanagan et al. (2002a,b) used 2,500 mg/L solutions at much higher application rates and found significant reductions in erosion, further suggesting the need for investigations into concentration and volume effects. Babcock and McLaughlin (2011) found significant reductions in turbidity and total suspended solids when PAM was applied to straw at a rate of 37 kg/ha and a concentration of 120 mg/L. In their study, the plots were on steep slopes (2:1) on construction sites and were not irrigated, so the PAM was allowed to dry before the first storm. Vacher et al. (2003) found increasing PAM rates tended to increase infiltration and reduce erosion in a rainfall simulator study, but viscosity issues with the high-molecular weight PAMs required up to 285 m^3/ha (34,000 gal/ac) spray volume to apply using hand sprayers. This volume is roughly five times the volume typically used for hydroseeding, so the effects using

commercial equipment, which can apply much more viscous solutions, may not be the same. Lu et al. (2002) evaluated PAM adsorption to soil materials collected from the upper 10 cm of six different soil series with a wide range of characteristics using PAM concentrations between 0 and 40 mg/L. They determined that PAM has a high affinity to be adsorbed by soil particles. However, because of its molecular size, it can only be adsorbed to the outer surface of soil particles, making its penetration into the soil profile highly dependent on the soil texture. In another study, Lu and Wu (2003b) examined PAM penetration into repacked columns (5.2 cm diameter) of soil materials collected from the upper 15 cm of two different soils. In their study, they removed the organic matter of the soil materials by combustion, and used PAM concentrations between 10 and 40 mg/L. Based on their results, they concluded that PAM can move into soils that contain no organic material, but its depth of penetration is limited to the upper part of the soil profile. Although these later studies address PAM adsorption and transport into soils of different textures, the soil materials that were used were from surface layers (i.e. low clay content) and the PAM concentrations were 10-fold lower than realistic field application rates used for erosion control at construction sites. The study here was intended to address key questions regarding the effectiveness of PAM applied to exposed soil at construction sites as affected by application rate and concentration. Specific objectives were:

(1) To evaluate the turbidimetric method using hyamine for determining PAM concentration in soil extract samples (***hyamine test***).

(2) To determine the effects of applied PAM formulations (dissolved vs granular) on runoff water quality, eroded sediment particle size distribution, and PAM loss by runoff (***runoff experiment***).

(3) To investigate the infiltration and transport of dissolved PAM through repacked soil columns (***column experiment***).

2. Materials and Methods

2.1. Hyamine test

2.1.1. PAM Materials

Three high-molecular weight (15 to 16 Mg mol^{-1}) anionic PAMs (Superfloc, Kemira Chemicals, Inc., Atlanta, GA) with a range of charge density were selected for study (Table 2.1). Stock solutions of PAM (1.0 g L^{-1}) were prepared by adding granular PAM to DI water and stirring for at least 24 h at room temperature. A 3.5% w/v hyamine solution was prepared by dissolving 3.5 g of benzethonium chloride (Hyamine 1622; Acros Organics, NJ) in 100 mL of DI water.

Table 2.1. Properties of anionic polyacrylamide (PAM) formulations used in this study.

PAM	Molecular weight	Charge density
	Mg mol^{-1}	mol %
A150	16	50
A120	15	20
A100	15	7

2.1.2. Soil extract preparation

Four NC soils, a Piedmont clay loam (PCL), a Piedmont sandy loam (PSL), a Coastal Plain sand (CPS), a Coastal Plain muck (CPM), were used to represent a range of textures and organic matter contents (Table 2.2). Three were mineral soils with high clay (PCL), high silt (PSL) or

high sand (CPS) contents, and one was mineral-organic soil with a high OM content (CPM). The CPM was surface soil (0-15 cm) from an agricultural field and the other three were fill soil materials from construction sites (surface and subsurface mixed). All soil materials were air-dried and passed through a 2-mm sieve. Soil extracts were obtained by equilibrating each soil with DI water for 24 h at 1:20 soil to solution ratio in an end-to-end shaker. After equilibration, the suspensions were centrifuged and the supernatant was decanted for use in experiments and further analysis. The soil extracts were analyzed for Al, Fe, Ca, Mg, K, and Na by inductively coupled plasma atomic emission spectroscopy (PerkinElmer, Waltham, MA), TOC with a Shimadzu carbon analyzer (Shimadzu Corp., Tokyo), and electrical (EC) conductivity with an EC Tester (Oakton instruments, Vernon Hills, IL). The results are presented in Table 2.3.

Table 2.2. Selected soil properties of Piedmont clay loam (PCL), Piedmont sandy loam (PSL), Coastal Plain sand (CPS), and Coastal Plain muck (CPM).

Property	Soil material			
	PCL	PSL	CPS	CPM
Texture	clay loam	sandy loam	sand	sandy loam
Sand[a] (g kg^{-1})	412	524	900	685
Silt[a] (g kg^{-1})	219	339	50	285
Clay[a] (g kg^{-1})	369	137	50	30
pH[b]	5.3	5.1	7.1	4.4
Organic matter[c] (g kg^{-1})	9.5	4.4	1.5	143.6

[a] Particle size analysis by hydrometer method.
[b] pH by a glass electrode at 1:1 soil to solution ratio.
[c] Organic matter by loss-on-ignition.

Table 2.3. Selected chemical properties of soil extracts.

Property	Soil extract[a]			
	PCL	PSL	CPS	CPM
EC[b] (µS/cm)	17	13	46	80
TOC[c] (mg L^{-1})	1.9	2.9	4.2	60
Al (mg L^{-1})	<0.01	3.00	3.00	2.30
Fe (mg L^{-1})	<0.01	1.50	1.90	0.31
Ca (mg kg^{-1})	1.20	0.08	7.00	5.30
Mg (mg kg^{-1})	0.48	0.20	0.44	1.70
K (mg kg^{-1})	0.19	0.50	0.63	3.60
Na (mg kg^{-1})	0.49	2.00	0.34	0.92

[a] Piedmont clay loam (PCL), Piedmont sandy loam (PSL), Coastal Plain sand (CPS), and Coastal Plain muck (CPM).
[b] Electrical conductivity.
[c] Total organic carbon.

2.1.3. Turbidimetric method using hyamine (hyamine test)

Solutions containing a range of PAM concentrations (0.5, 1, 2.5, 5, 10, 25, and 50 mg L^{-1}) were prepared in either DI water or soil extract. A 10 mL aliquot of PAM solution at each concentration was transferred to a 15-mL conical tube and 100 µL of hyamine solution was then added to the tube. The sample was mixed by shaking for 10 s. After a 5 min reaction (waiting)

time, the turbidity was measured using a portable turbidimeter (LaMotte Company, Chestertown, MD) in nephelometric turbidity units (NTU). Our preliminary results in DI water indicated that PAM concentrations ≤ 0.5 mg L^{-1} did not yield enough turbidity upon hyamine addition to be distinguished from blank solutions.

2.1.4. PAM calibration curve and method validation

Using the turbidity readings obtained by the hyamine-PAM reaction, PAM calibration curves (plots of PAM concentration vs. turbidity) were constructed individually as a factorial combination of three anionic PAMs, five solution compositions (DI water and four soil extracts), and seven concentration levels (0.5, 1, 2.5, 5, 10, 25, and 50 mg L^{-1}). All combinations were performed in triplicate and the mean values were used to develop the PAM calibration curves.

For the analytical method validation, we determined signal detection limit, minimum detectable concentration (C_{md}), linearity, and sensitivity. Signal detection limit (y_{dl}) is the highest analytical signal (NTU) when replicates of a sample containing no analyte are tested, and it was determined by (Harris, 2007)

$$y_{dl} = y_{blank} + 3\sigma \quad [1]$$

where y_{blank} is the mean turbidity signal (NTU) of blank solutions containing hyamine but no PAM (n = 8) and σ is the standard deviation (n = 8) of turbidity in low PAM concentration samples (0.5 mg L^{-1}). Assuming a Gaussian distribution of the raw analytical signals from blank samples, the y_{dl} represents 99% of the observed values and the remaining 1% represents a response that could be produced by a sample containing a very low concentration of analyte (Armbruster and Pry, 2008). The corrected signal (y_{sample} - y_{blank}) was used to construct a PAM calibration curve by

$$y_{sample} - y_{blank} = m \times C \quad [2]$$

where y_{sample} is the mean turbidity signal (NTU) of PAM solutions reacted with hyamine (n = 3), m is the slope of the linear calibration curve, which is a measure for the sensitivity of the calibration curve, and C is PAM concentration (mg L^{-1}) in the sample. Data were subjected to regression analysis using the least square method. For each regression model, coefficient of determination (r^2) and residual standard deviation (*RSD*) were estimated to assess the linearity and deviation of the data from the fitted regression line by using the data analysis package within Microsoft excel 2010 (Kuss, 2003). Significance of the linear regression model was determined with p-value for the F-test in the analysis of variance. The C_{md}, often called as detection limit, was obtained by substituting y_{dl} from Eq. [1] for y_{sample} in Eq. [2]:

$$C_{md} = 3\sigma / m \quad [3]$$

2.2. Runoff Experiment

2.2.1. Runoff box preparation and treatments

Soil material was collected from an excavation (surface and subsurface mixed) at a local construction site in the Piedmont region of NC. The soil texture was a sandy clay loam (41% sand, 22% silt, and 37% clay) with a pH of 5.3. The soil was air-dried, passed through a No. 25-mesh (7.1 mm) sieve and packed in wooden boxes, 100 cm long, 20 cm wide and 5 cm deep (Fig. 2.1). Each box had three 5-mm drainage holes in the base to allow drainage during rainfall simulations. The bottoms of the boxes were covered with a layer of cheese-cloth before packing

13.2 kg of soil into each box to achieve a bulk density of 1.5 g cm^{-3}. The final depth of soil was approximately 4.5 cm.

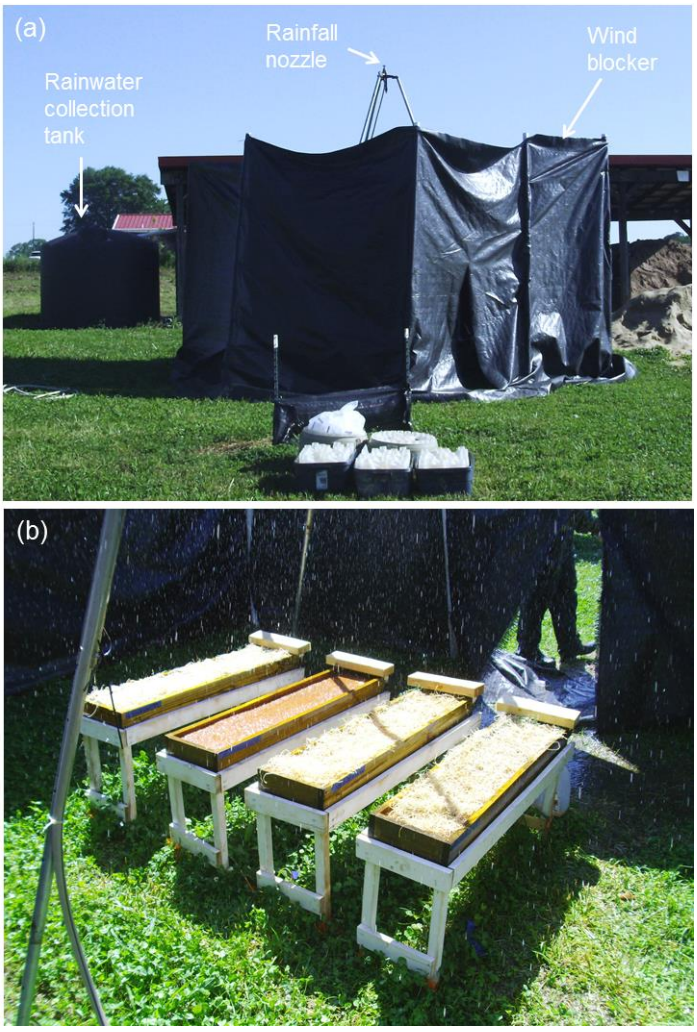

Figure 2.1. Setup of rainfall simulation tests showing (a) exterior view and (b) interior view.

A total of four treatments were included in the study: 1) no cover + no PAM (bare soil; control), 2) cover + no PAM, 3) cover + GPAM, and 4) cover + DDPAM. The cover material was an excelsior blanket (American Excelsior Company, Rice Lake, WI), which is one of the commonly used ECBs in NC. The excelsior blanket was cut to cover the whole soil surface area in the boxes (Fig. 2.1). We used a high molecular weight, anionic (50% charge density) PAM (Superfloc A150, Kemira Chemicals Inc., Atlanta, GA). Jar tests indicated that A150 PAM flocculated the study soil well and that A150 PAM had high sensitivity for detection using a turbidimetric detection method (Kang et al., 2013a). One day before rainfall simulation, 1.2 L of DPAM at a concentration of 500 mg L^{-1} and 600 mg of GPAM were uniformly applied to the respective treatments at a recommended rate of 30 kg ha^{-1} for hydroseeder applications (Hayes et al., 2005). To create similar initial soil moisture conditions among treatments, the GPAM and no PAM treatments received same volume of water (1.2 L) as the DPAM treatment via a watering can. The excelsior blanket was installed after the PAM and water applications.

2.2.2. Rainfall simulation

Rainfall simulation was conducted at the Sediment and Erosion Control Research and Education Facility (SECREF) in Raleigh, NC. The source of water was natural rainwater collected from a building roof and stored in a tank until use. The rain water had a pH of 5.2 with background turbidity of 7 nephelometric turbidity units (NTU) (Table 2.4). A four-sided wind screen, constructed of plastic tarps, was placed around the rainfall simulator to minimize wind effects on rainfall distribution (Fig. 2.1). Four soil boxes with randomly assigned treatments were placed under the rainfall simulator on a stand having a 5% slope for each of two rainfall simulations (i.e., 2 replications), with new soil used in each replication. A single nozzle (FullJet, 1/2HH-SS50WSQ, Spraying System Company, Wheaton, IL) was located 3 m above the boxes and applied rainwater at a constant rainfall intensity of 8.3 cm h^{-1}. Each rainfall simulation consisted of two subtests (hereafter referred to as events). The first event was 50 min long and the second event was 20 min long. A 30-min rest period was allowed between the two events. The 30-min rest period was included to determine if the applied PAM remained effective in erosion and turbidity control for repeated storms. Total rainfall over both events was 9.7 cm, similar to a 2-h, 100-year storm event for this region (NCDENR, 2006). Surface runoff exited the soil box through a gutter and was directed into a rubber hose that funneled the runoff into a collection container. The collection gutter at the lower end of the boxes was protected by a shield to prevent rainfall from entering the collection container.

Table 2.4. Chemical properties of the water used for rainfall simulation.

Property	Value
pH	5.2
EC (µS cm^{-1})	13
Turbidity (NTU)	7.1
Total suspended solid (mg L^{-1})	15
Total organic carbon (mg L^{-1})	1.70
Al (mg L^{-1})	<0.01
Ca (mg L^{-1})	0.36
Fe (mg L^{-1})	<0.01
K (mg L^{-1})	0.18
Mg (mg L^{-1})	0.13
Na (mg L^{-1})	0.11

For each event, time for runoff initiation was recorded as elapsed time between the start of rainfall and the time at which surface runoff began entering runoff collection container. Runoff was sampled at 5-min intervals and its volume was measured. Runoff rate (mm h^{-1}) was calculated as (runoff volume)/(sampling interval × box surface area) after runoff initiation. Collected samples were analyzed for turbidity using an Analyte NEP turbidity probe (McVan Instruments, Melbourne, Australia) and TSS concentration after filtering through 76-mm fiberglass filters and drying for 24 h at 105 °C (Clesceri et al., 1998). Concentrations of PAM in runoff water were determined turbidimetrically using a cationic surfactant (hyamine 1622) according to the procedures in Kang et al. (2013a). Mean runoff TSS, turbidity, and PAM concentration of two replicated tests were used for data presentation. Erosion rate (kg ha^{-1} h^{-1}) was calculated as (TSS concentration × runoff volume)/(sampling interval × box surface area).

2.2.3. Particle size distribution

Runoff samples from one replication for each treatment were analyzed for particle size distribution via a laser diffraction (LD) particle size analyzer (LS 13 320 Series, Beckman Coulter, FL). The suspensions of runoff samples were introduced to the LD analyzer while being stirred by a magnetic bar. The analyzer determines volumetric particle size distribution by measuring the pattern of light scattered by the particles in the sample. The scattering intensity data were analyzed to calculate the size of the particles responsible for creating the scattering pattern, using the Mie theory of light scattering (Agrawal et al., 1991; Eshel et al, 2004). The analyzer had a detection range between 0.04 μm and 2 mm and the particle size was reported as a volume-based sphere diameter.

Statistical analysis

Analysis of variance (ANOVA) was used to determine treatment effects on runoff rate, turbidity, TSS concentration, and erosion rate by setting these dependent variables as repeated measurements. One-way ANOVA for individual treatments and two-way ANOVA (cover and PAM) were run using the PROC GLM procedure in SAS (Version 9.3; SAS Institute, Cary, NC). The effect of sampling time was insignificant ($p > 0.05$), so it was not included as a treatment factor. Statistical differences between treatments were tested with Waller-Duncan K-ratio *t* Test at a probability level of 0.05 (SAS, 2011).

2.3. Column Experiment

2.3.1. Soil column setup

The soil material was a sandy clay loam (41 % sand, 22 % silt, and 37 % clay) with a pH of 5.3 and it was collected from an excavation (surface and subsurface mixed) of a local construction site at the Piedmont region of NC. The soil was air-dried and passed through a 2-mm sieve, and mixed thoroughly before use. A total of 10 soil columns (7.56-cm long and 7.56-cm wide metal cylinder) were packed with 121 g of sieved soil to a bulk density of 1.3 g cm^{-3} and the thickness of the soil layer in the columns was 2 cm (Fig. 2.2). Double-layers of cheese cloth were placed at the bottom of soil and a single layer was placed on the top of soil surface. The soil columns were then wetted from below with deionized (DI) water until saturation.

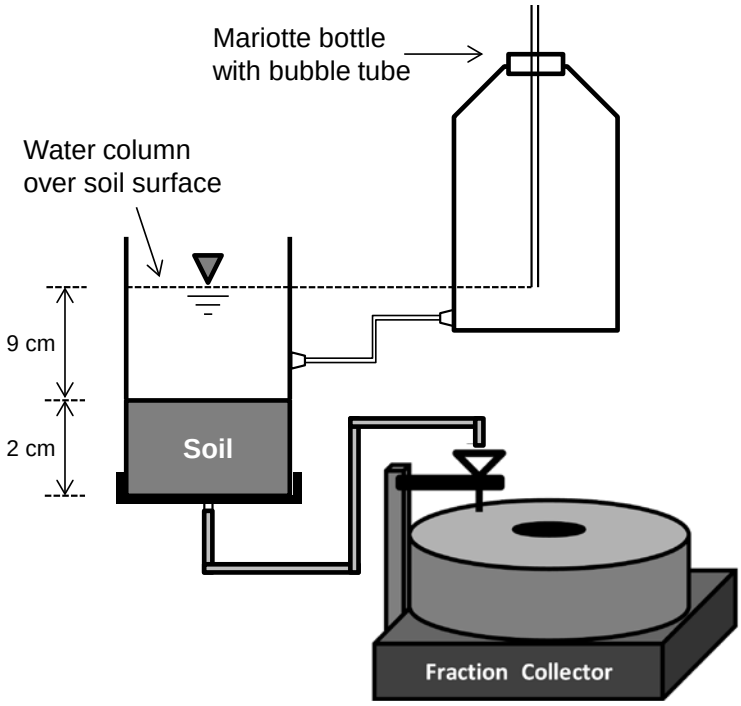

Figure 2.2. Schematic diagram of hydraulic conductivity measurement and polyacrylamide displacement tests.

Following saturation, the saturated columns were placed on a wooden rack with drain funnels and an empty metal cylinder was connected to the top of each column using a large rubber land. The columns were then leached from the top with DI water according to the constant-head method for hydraulic conductivity (HC) of saturated soil (Klute, 1986). After the water level on the top of sample has become stabilized (≈ 9 cm), the leachate was sampled at least three times. The HC (cm d^{-1}) was determined by measuring the volume of leachate Q that pass through the soil sample in a known time t:

$$HC = (Q / At)\ (L/\Delta H) \quad [4]$$

where A is the cross-sectional area of the soil sample (45.6 cm^2), L is the length of the sample (2 cm), and ΔH is the head difference across the sample (11 cm). These readings were taken as initial HC values prior to PAM addition at $t = 0$. The HC measurement continued during the PAM displacement tests.

2.3.2. PAM displacement test

The PAM used for this study was a high molecular-weight, anionic polymer with 50 mol % of charge density (Superfloc A150, Kemira Chemicals Inc., Atlanta, GA). The PAM flocculated the study soil well and had high analytical sensitivity in measuring dissolved PAM concentration turbidimetrically due to its higher charge density (Kang et al., 2013a). Stock solution of the PAM (500 mg L^{-1}) was made in DI water and stirred for at least 24 h at room temperature.

We selected two columns that had the most similar HC at $t = 0$ for further tests to investigate the PAM displacement through 2-cm soil layer by two different PAM application modes: 1) pulse input and 2) step input. For the pulse input, 27 mL of 500 mg L^{-1} of dissolved PAM was applied by pipette after removing the ponded water without breaking saturated condition. This allowed us to have relative PAM concentration (C/C_o) in leachate against input concentration of 500 mg

L^{-1}. Upon the end of dissolved PAM infiltration onto the soil, water input was switched to DI water and maintained saturated condition under the constant head. The step input was continuous application of 25 mg L^{-1} of dissolved PAM without switching to the DI water.

Breakthrough curve data were fitted with an analytical solution of a physical nonequilibrium model or two-region model, which is based on a dual-porosity concept. Equilibrium convective-dispersive equation (CDE) model based on a single porosity was poorly fitted to the measured data. In the two-region model, water-filled pore space is divided into two regions, mobile and immobile liquid region. Convective-dispersive transport is confined to the mobile liquid region while the presence of a solute in an immobile region within an aggregate is dependent on diffusion from the mobile to the immobile liquid. One-dimensional transport of reactive solute during steady-state flow is written as (Lal and Shukla, 2004):

$$\theta = \theta_m + \theta_{im} \quad [5]$$

$$\theta_m \frac{\partial c_m}{\partial c_t} + f\,\rho_b \frac{\partial s_{sm}}{\partial t} + \theta_{im} \frac{\partial c_{im}}{\partial t} + (1-f)\rho_b \frac{\partial s_{im}}{\partial t} = \theta_m D_m \frac{\partial^2 c_m}{\partial x^2} - \theta_m v_m \frac{\partial c_m}{\partial x} \quad [6]$$

$$\theta_{im} \frac{\partial c_{im}}{\partial t} = \alpha(C_m - C_{im}) \quad [7]$$

where θ_{im} and θ_m are volumetric water content of mobile and immobile liquid phases, C_m and C_{im} are concentrations in mobile and immobile phases, t is time, D_m is dispersion coefficient of mobile phase, v_m is the average mobile pore water velocity, x is depth, α is chemical mass transfer coefficient between mobile and immobile liquid phases. Note that for the two-region model, pore water velocity (v) = ($\theta_m v_m$)/ θ and dispersion coefficient (D) = ($\theta_m D_m$)/ θ.

At the end of displacement tests, soil samples in the columns were weighted to determine volumetric water content (θ) in triplicates, which is equal to water-filled porosity (f) in saturated column (Hillel, 2004). The average value of f was 0.36 ± 0.001 (mean ± std. error) and column pore volume at saturation was determined to be 33.2 cm^3 by:

$$V_o = V_t \times f \quad [8]$$

where V_t is the total volume of soil (cm^3). The number of pore volumes (PV) for column leachate was determined by:

$$PV = V_c/V_o \quad [9]$$

where is the cumulative volume of leachate (cm^3). Data from the tests were plotted with relative concentration (C/C_o) of leachate PAM as a function of dimensionless time, PV. The data were then analyzed using the computer program CXTFIT that estimate solute transport parameters from measured breakthrough curves using a non-linear least-squares fitting procedure (Toride et al., 1999). Inverse module in the CXTFIT was used to estimate retardation factor (R), D, β, and ω by fitting the parameters in an analytical solution to the two-region CDE (Eq. 5-7). The parameters β and ω are dimensionless expressions of the mobile water and the mass transfer coefficient, respectively (Hebert Jr., 2011):

$$\beta = \theta_m/\theta \quad [10]$$

$$\omega = (\alpha L)/(\theta v) \quad [11]$$

where L is the characteristic length of the studied system (column length). The parameter β represents the fraction of solute present in the mobile region under equilibrium conditions while ω represents the ratio between hydrodynamic residence time and a characteristic time of solute movement in the immobile region. The two-region model becomes to a one-region, one porosity model when β =1. Solute concentrations in the mobile and immobile phases are in equilibrium for high values of ω (>100) whereas mass transfer between mobile and immobile phases becomes insignificant at very low value of ω (≈ 0). For our CXTFIT simulations, relative concentrations of PAM (C/C_o), application mode (pulse or step) and duration of influent PAM, average *v* were entered in as known parameters. The average *v* for each column was determined by:

$$v = (q/A) / \theta \quad [12]$$

where *A* is the cross-sectional area of the column (cm^2).

Leachate samples were collected via a fraction collector (Fig. 2.2) and the samples were composited to make up enough volume (100 mL) for the determination of PAM. Concentrations of PAM were determined turbidimetrically using a cationic surfactant (hyamine 1622) according to the procedures in Kang et al. (2013a). Sample collection lasted up to 3 days (29 *PV*) for the column with pulse input and up to 47 days (181 *PV*) for the column with step input.

2.3.3. PAM sorption isotherm

Polyacrylamide adsorption was measured and an isotherm was constructed to estimate Langmuir-model parameters for the study soil material according by conventional batch technique. Briefly, 1.5 gram of soil sample was equilibrated in centrifuge tubes with 30 mL of PAM solutions with initial PAM concentrations at 0, 0.5, 1, 2.5, 5, 10, 25, 50, 75, 100 mg L^{-1}. The tubes were shaken for 24 h on a reciprocating shaker, centrifuged (5 min at 15,000 rpm), and the supernants were decanted off for further PAM analysis. The PAM sorption parameters were determined with a linearized form of the Langmuir equation:

$$C/S = C/S_{max} + 1/(K_L S_{max}) \quad [13]$$

where *C* is the concentration of PAM in solution after the 24-h equilibration (mg L^{-1}), *S* is the amount of PAM adsorbed by soil (mg kg^{-1}), S_{max} is the Langmuir PAM sorption maxima (mg kg^{-1}), and K_L is an affinity constant related to binding energy (L mg^{-1}). Model parameters were estimated from a linear regression of *C*/*S* against *C*, where the slope equals $1/S_{max}$ and the intercept equals $1/(K_L S_{max})$.

Adsorption partition coefficient, often referred to as distribution coefficient (k_d, L kg^{-1}), is a ratio adsorbed phase concentration to the solution phase concentration at equilibrium and it is the slope of the Langmuir isotherm at any point (Fetter, 1999). Values of k_d was determined by solving for S in eq. [13] and differentiating it with respect to C (Akhtar et al., 2003):

$$k_d = \frac{dS}{dC} = \frac{1}{1+K_L C}\left[K_L S_{\max} - \frac{K_L{}^2 S_{\max} C}{1+K_L C}\right] \quad [14]$$

The value of k_d over *C* was used to estimate the retardation factor for PAM given equilibrium PAM concentration (*C*):

$$R = 1 + (\rho_b k_d)/\theta_w \quad [15]$$

where ρ_b is the soil bulk density (g cm^{-3}).

3. Results and Discussion

3.1. Hyamine test

3.1.1. PAM calibration curves in DI water matrix

All anionic PAMs yielded strong linear relationships between turbidity and PAM concentration with the $r^2 \geq 0.99$ (Fig. 3.1; Table 3.1). As seen in the increasing slopes, the sensitivity of the hyamine test increased with increasing charge density of the anionic PAMs. The C_{md} for the highest charge density PAM (0.4 mg L^{-1}) was less than half that of the PAM with the lowest charge density (0.9 mg L^{-1}). Our results are thus in agreement with Allison et al. (1987) who found similar dependence of sensitivity on charge density of anionic PAMs in brine solutions.

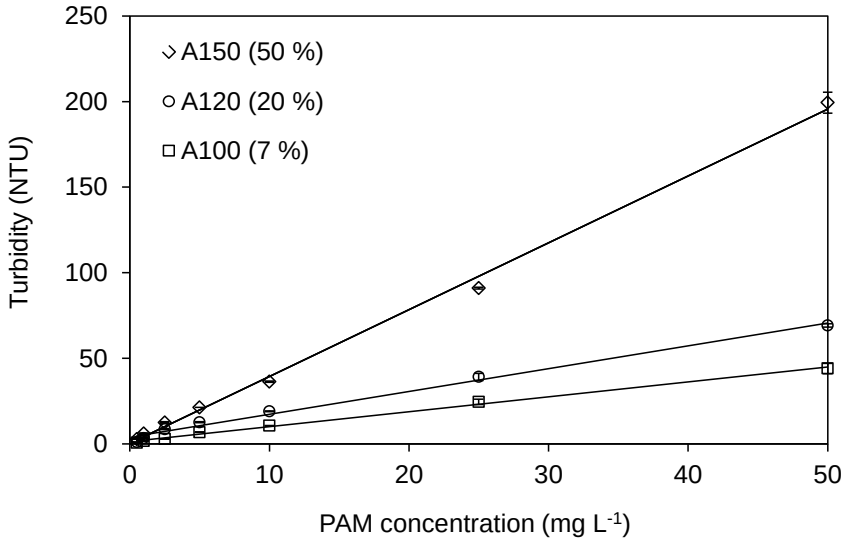

Figure 3.1. Polyacrylamide (PAM) calibration curves in deionized water. Charge density (mol %) for each PAM formulation is shown in parenthesis. Error bars are the standard error of the three replicates.

Table 3.1. Hyamine method analytical parameters in deionized water for each polyacrylamide (PAM) formulation.

	PAM		
	A150	A120	A100
Minimum detectable signal y_{dl} (NTU)	2.3	1.8	1.4
Minimum detectable concentration C_{md} (mg L^{-1})	0.4	0.8	0.9
Sensitivity (regression slope m ± std. error, NTU L mg^{-1})	3.91 ± 0.06	1.44 ± 0.07	0.90 ± 0.02
Coefficient of determination (r^2)[a]	0.99***	0.99***	0.99***
Residual standard deviation (NTU)	3.74	4.02	1.47

[a] The symbols *, **, and *** indicates statistical significance of regression model at the 0.05, 0.01, and 0.001 level respectively.

3.1.2. PAM calibration curves in soil extracts

The background turbidity in soil extracts (i.e., with no PAM added and before the hyamine addition) varied by soil materials. For instance, PCL extract had the lowest background turbidity (2.2 ± 0.3 NTU) whereas those of other soil extracts ranged from 8.3 to 11.7 NTU (Table 3.2). The relatively higher background turbidity in PSL and CPS than PCL was most likely attributed to the difference in chemical/mineralogical composition, including differences in clay-sized fraction (McLaughlin and Bartholomew, 2007) and increase in the TOC in the suspension (Lu and Wu, 2001). Upon addition of hyamine, PSL and CPS extracts in the absence of PAM yielded 2- to 3-fold greater readings in turbidity compared to their background turbidity. The extreme case was observed with the CPM blank solution, which yielded 30-fold greater turbidity development compared to its background turbidity. High TOC in the CPM extract (60 mg L^{-1}) likely reacted with hyamine in a manner analogous to PAM, producing high turbidity which could interfere with PAM detection. This result implied that the hyamine test is only useful in solutions with relatively low organic carbon, as discussed later more in detail. The sensitivity (as shown by the slope *m*) of the hyamine test varied not only with the charge density of PAMs but also with the type of mineral soil extract (PCL, PSL, and CPS) (Fig. 3.2; Table 3.3). For example, *m* for A150 PAM ranged from 3.47 to 3.90 (NTU L mg^{-1}); *m* for the PCL was the greatest and comparable to the *m* in DI water (3.91 NTU L mg^{-1}). As seen in trials in DI water (Fig. 3.1), the sensitivity of the hyamine method in soil extracts decreased with decreasing charge density. The method sensitivity in PSL and CPS was diminished compared to that of DI water, particularly with A120 and A100 PAMs. By comparing the values across soil extracts, it appears the high charge density PAM (A150) was least affected by soil extract types, having a consistently low C_{md} value of 0.3 to 1.2 mg L^{-1}.

Table 3.2. Turbidity (mean ± std. dev.) of blank samples in deionized (DI) water and soil extracts before and after hyamine addition.

	Turbidity				
		Soil extract[a]			
Hyamine	DI water	PCL	PSL	CPS	CPM
		NTU			
Before	0.1 ± 0.2	2.2 ± 0.3	11.7 ± 0.3	8.3 ± 0.4	10.5 ± 2.2
After	0.6 ± 0.3	2.7 ± 0.4	22.5 ± 1.6	25.9 ± 0.9	298 ± 35

[a] Piedmont clay loam (PCL), Piedmont sandy loam (PSL), Coastal Plain sand (CPS), and Coastal Plain muck (CPM).

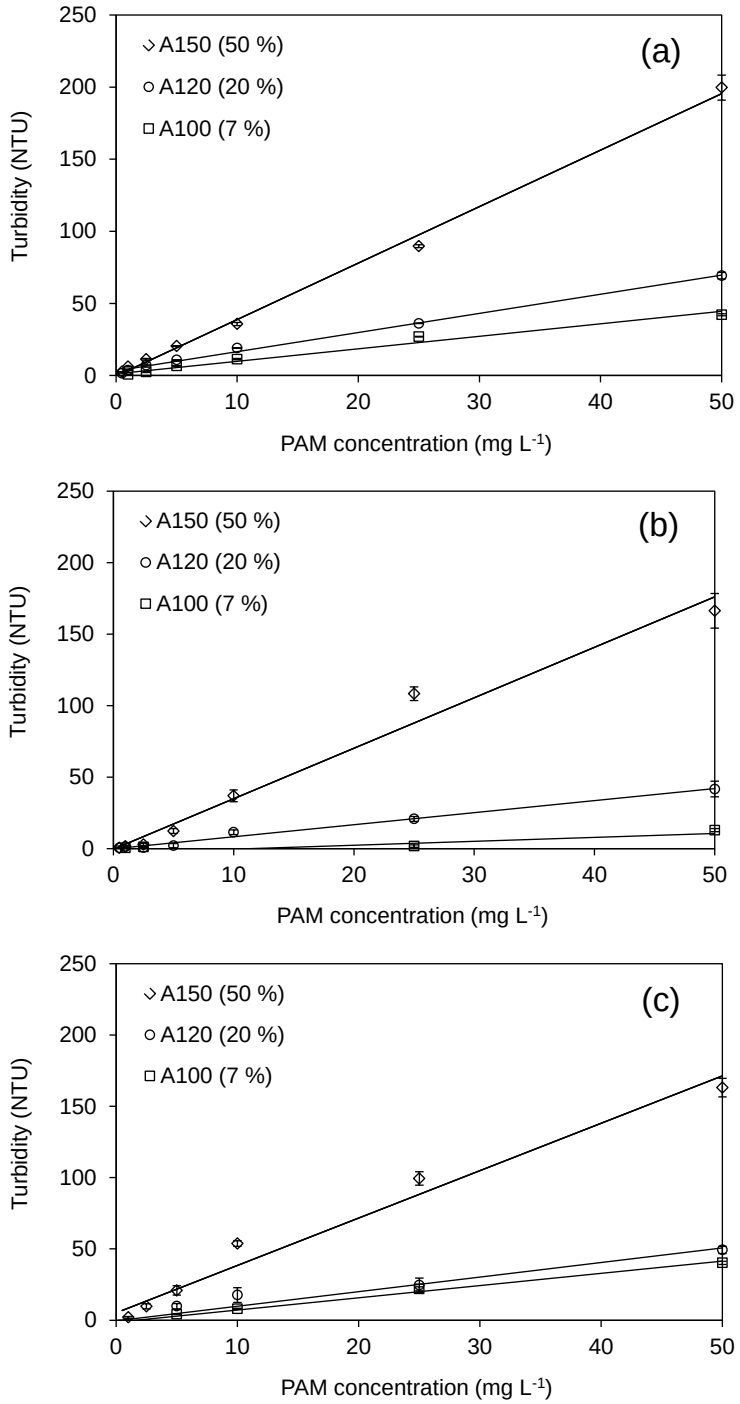

Figure 3.2. Polyacrylamide (PAM) calibration data in the Coastal Plain muck extract for three PAMs (A150, A120, and A100). Charge density (mol %) for each PAM is shown in parenthesis. Error bars are the standard error of the three replicates.

Table 3.3. Hyamine method analytical parameters in soil extracts for each polyacrylamide (PAM) formulation.

	Piedmont clay loam			Piedmont sandy loam			Coastal Plain sand		
PAM formulation	A150	A120	A100	A150	A120	A100	A150	A120	A100
Minimum detectable signal y_{dl} (NTU)	3.9	3.7	4.8	24.2	25.8	27.5	30.0	33.2	33.1
Minimum detectable concentration C_{md} (mg L^{-1})	0.3	0.7	2.4	0.5	4.0	22.7	1.2	7.2	8.8
Sensitivity (regression slope m ± std. error, NTU L mg^{-1})	3.90 ± 0.07	1.42 ± 0.06	0.90 ± 0.04	3.52 ± 0.17	0.84 ± 0.03	0.18 ± 0.08	3.47 ± 0.18	1.01 ± 0.08	0.82 ± 0.03
Coefficient of determination (r^2)[a]	0.99***	0.99***	0.98***	0.99***	0.99***	0.44*	0.98***	0.96***	0.99***
Residual standard deviation (NTU)	4.14	3.15	2.53	9.82	1.63	4.81	10.4	4.90	1.94

[a] The symbols *, **, and *** indicates statistical significance of regression model at the 0.05, 0.01, and 0.001 level respectively.

There was no evidence of a turbidity response to increasing PAM concentrations in the CPM extract (Fig. 3.3). High blank turbidity in the CPM extract developed from reaction of hyamine with pre-existing organic carbon (Table 3.2) overwhelmed the turbidity response derived from dissolved PAM. The soil extracts from mineral soils all contained < 5 mg L^{-1} TOC, whereas the CPM extract had 60 mg L^{-1} TOC (Table 2.3). Furthermore, the blank turbidity caused by hyamine in mineral soil extracts (2.7 to 25.9 NTU) trended with measured TOC in the extracts (Table 5), suggesting that there is a maximum TOC concentration beyond which interference from TOC renders the test not useful. One approach to handling higher TOC from organic-rich soils would be to dilute the extract, which we did with the CPM extract (Fig. 3.4). Once the dilution reached 25-times, or 2.4 mg L^{-1} TOC (i.e., 25-times diluted from 60 mg L^{-1}), the CPM + hyamine solution yielded < 20 NTU, similar to the other soils. However, this would raise the C_{md} by the same factor, which may be unacceptable for applications needing greater sensitivity.

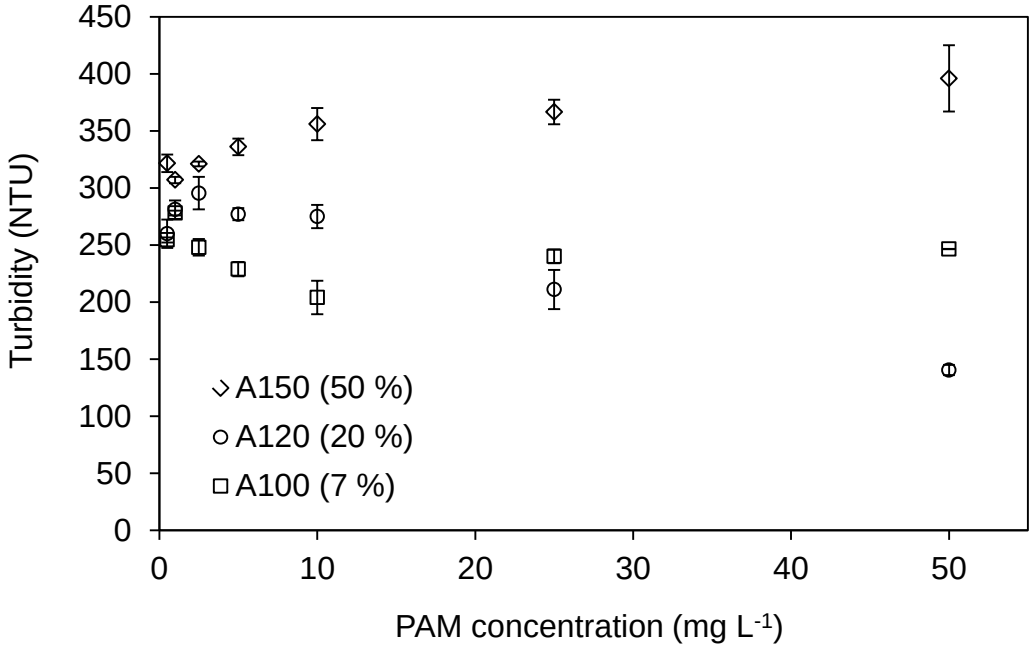

Figure 3.3. Polyacrylamide (PAM) calibration data in the Coastal Plain muck extract for three PAMs (A150, A120, and A100). Charge density (mol %) for each PAM is shown in parenthesis. Error bars are the standard error of the three replicates.

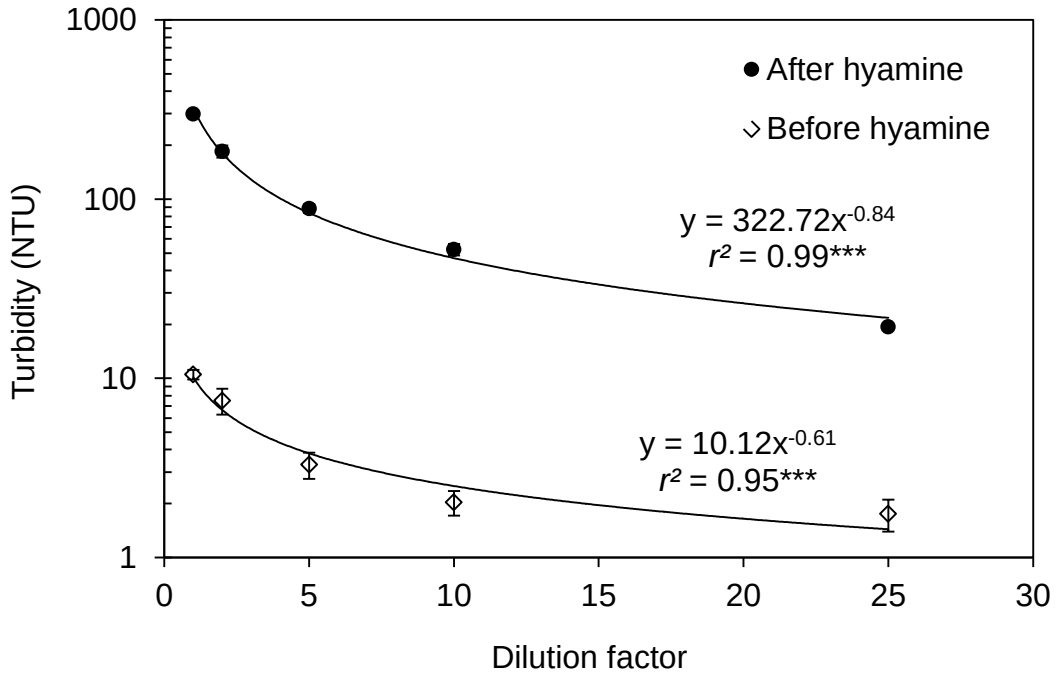

Figure 3.4. Turbidity development in Coastal Plain muck extract affected by dilution before and after hyamine addition. Error bars are the standard error of the three replicates. Note a logarithmic scale in Y-axis.

3.1.3. Summary

Rapid, simple, and inexpensive determination of PAM in solution could be a very useful tool for determining PAM's fate in environmental applications. Our results suggest that the turbidimetric method by hyamine is relatively simple and efficient in determining PAM concentration in soil extracts with low organic carbon (< 5 mg TOC L^{-1}). The hyamine test was not sensitive to PAM in the soil extracts with higher TOC (60 mg L^{-1}).

The results have significant implications for the application of this method for determining PAM in soil water samples. Because dissolved organic carbon appears to be a problematic interference, the method may be poorly suited to use for runoff samples containing high organic carbon, such as those found in agricultural settings. In contrast, the method has higher sensitivity and lower detection limit in extracts from mineral soils. This suggests that the method may be well suited for the quantification of PAM in runoff or leachate from construction sites, which often have low OM subsoils exposed at the surface. Because of the dependence of the signal on soil types, developing PAM calibration curves for the soil and anionic PAM of interest using hyamine test will be necessary for the determination of PAM in soil water samples from impacted areas.

3.2. Runoff Experiment

3.2.1. Runoff initiation and volume

During the first rainfall event, runoff was initiated 12 to 18 min after the start of rainfall (Table 3.4). The runoff rate was lower for cover + DPAM compared to other treatments (Fig. 3.5). Runoff was initiated immediately after rainfall in the second event for all treatments. Enhanced infiltration and runoff reduction from PAM applications have been reported under rainfall or irrigation simulations (Ben-Hur and Letey, 1989; Levy et al., 1992). Our results agree with the finding of Flanagan et al (2002a, b) who reported that application of DPAM in concentrations of up to 2,500 mg L^{-1} was effective in delaying runoff and reducing runoff volume if it was allowed to dry before irrigation. Visual observations of the soil in the cover + DPAM treatment indicated that the soil surface was relatively intact and there was less disturbance after rainfall simulations compared to the soil surface in the other treatments (Fig. 3.6). Our observations match with previous studies (Peterson et al., 2002; Shainberg et al., 2011; Babcock and McLaughlin, 2013) in that GPAM was less effective than DPAM in reducing runoff because the partially hydrated PAM granules tended to block soil pores and inhibit water infiltration during rainfall.

Table 3.4. Comparison of time to runoff initiation (TRI), runoff ratio over applied rainfall (runoff/rainfall), runoff rate, turbidity, total suspended solids (TSS) concentration, erosion rate affected by cover and polyacrylamide (PAM) treatments.

Variable	First rainfall event				Second rainfall event			
	No cover + No PAM	Cover + No PAM	Cover + GPAM[a]	Cover + DPAM[a]	No cover + No PAM	Cover + No PAM	Cover + GPAM[a]	Cover + DPAM[a]
TRI (min)	12.2	12.8	13.4	18.4	n.d.[b]	n.d.[b]	n.d.[b]	n.d.[b]
Runoff/rainfall (cm cm^{-1})	0.48	0.46	0.42	0.32	0.65	0.47	0.65	0.43
Turbidity (NTU)[c]	2,315 ± 50a	903 ± 64b	78 ± 9c	60 ± 6c	2,314 ± 92a	774 ± 95b	80 ± 17c	79 ± 18c
TSS (mg L^{-1})[c]	2,670 ± 74a	1,039 ± 208b	79 ± 5c	69 ± 12c	3,417 ± 461a	883 ± 234b	67 ± 3c	55 ± 9c
Erosion rate[c] (kg ha^{-1} h^{-1})	1,460 ± 97a	435 ± 69b	41 ± 6.5c	24 ± 1.7d	1,764 ± 236a	527 ± 173b	38 ± 2.8c	24 ± 4.6c

[a] GPAM = granular PAM; DPAM = dissolved PAM.

[b] n.d. = no delay.

[c] Mean values averaged over time (mean ± std. error). Values followed by different letters within a row for each rainfall are significantly different ($p < 0.05$).

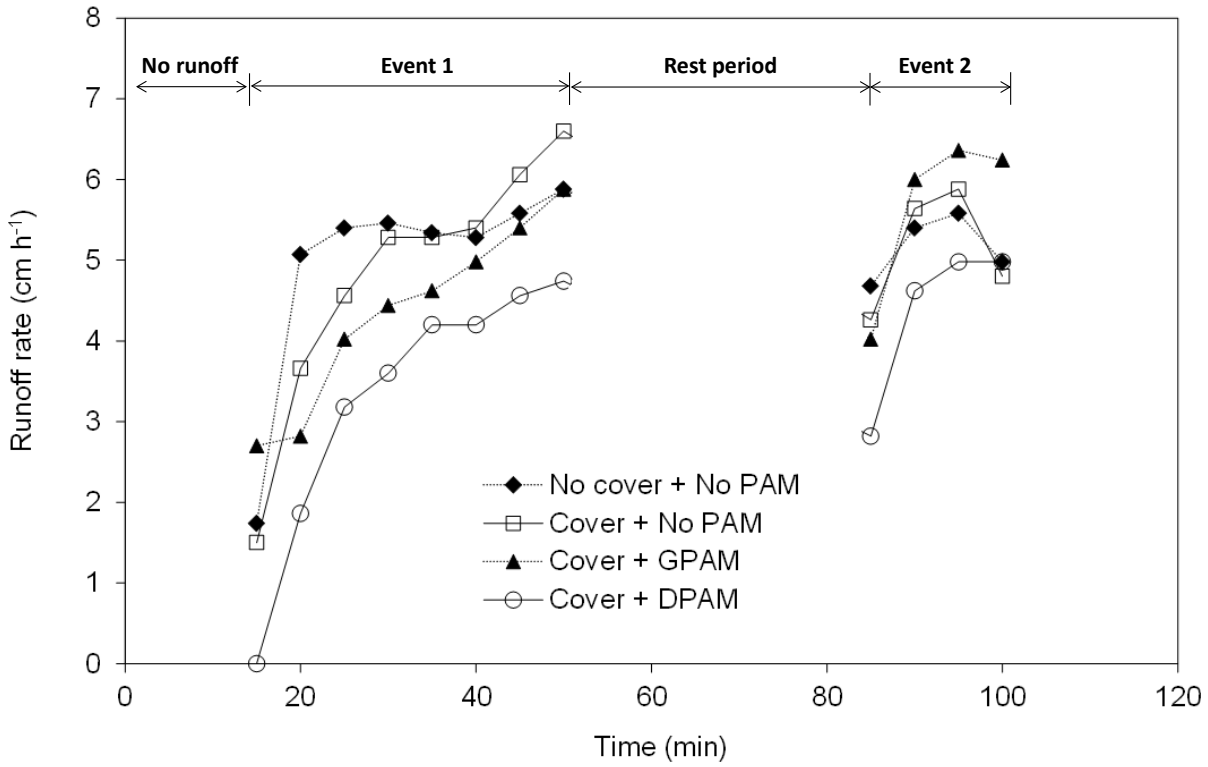

Figure 3.5. Comparison of runoff rate over the first (0 to 50 min) and second (80 to 100 min) rainfall events with a 30-min rest period between rainfall events. The GPAM and DPAM are granular and dissolved polyacrylamide (PAM), respectively.

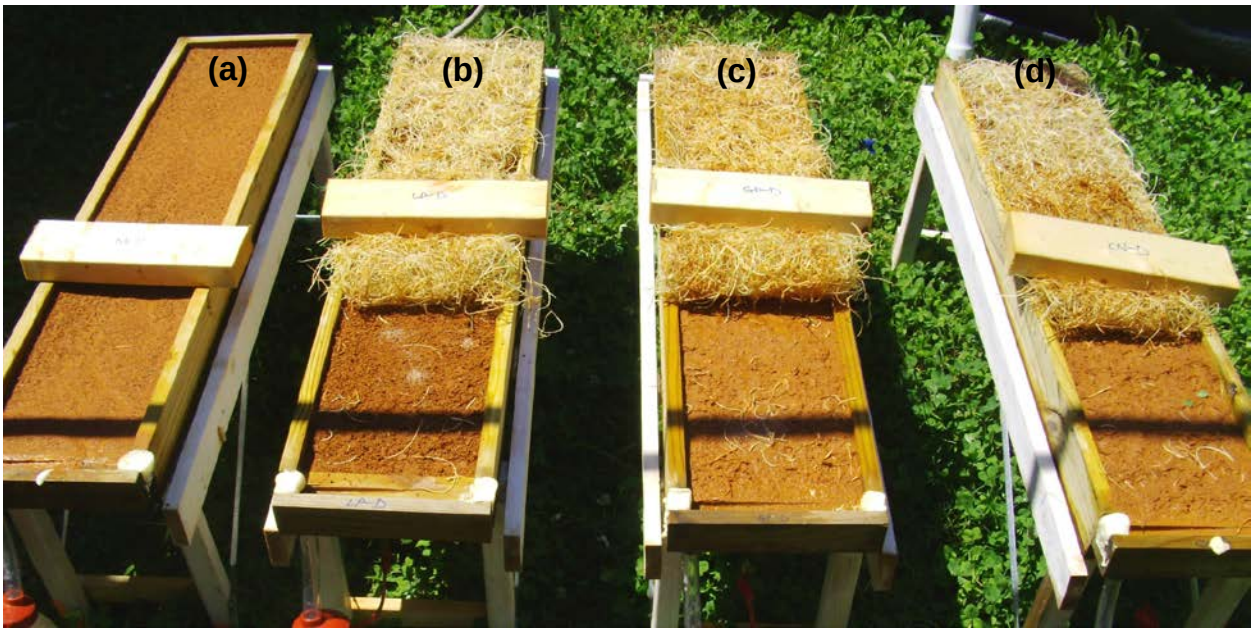

Figure 3.6. Soil surfaces in runoff boxes after rainfall simulations: (a) no cover + no PAM, (b) cover + DPAM, (c) cover + GPAM, and (d) cover + no PAM. GPAM and DPAM are granular and dissolved polyacrylamide (PAM), respectively.

3.2.2. Turbidity and sediment

Both surface cover and PAM had significant effects on turbidity and TSS in runoff during the first and second rainfall events ($p < 0.001$). Cover alone reduced turbidity and TSS to less than half of that compared to no cover (Table 3.4). Adding GPAM and DPAM with the cover reduced turbidity (< 80 NTU) and TSS (< 80 mg L^{-1}) by more than an order of magnitude. There was a clear separation between the PAM-treated boxes and the others from the beginning of the tests, which continued through the second rainfall event (Fig. 3.7).

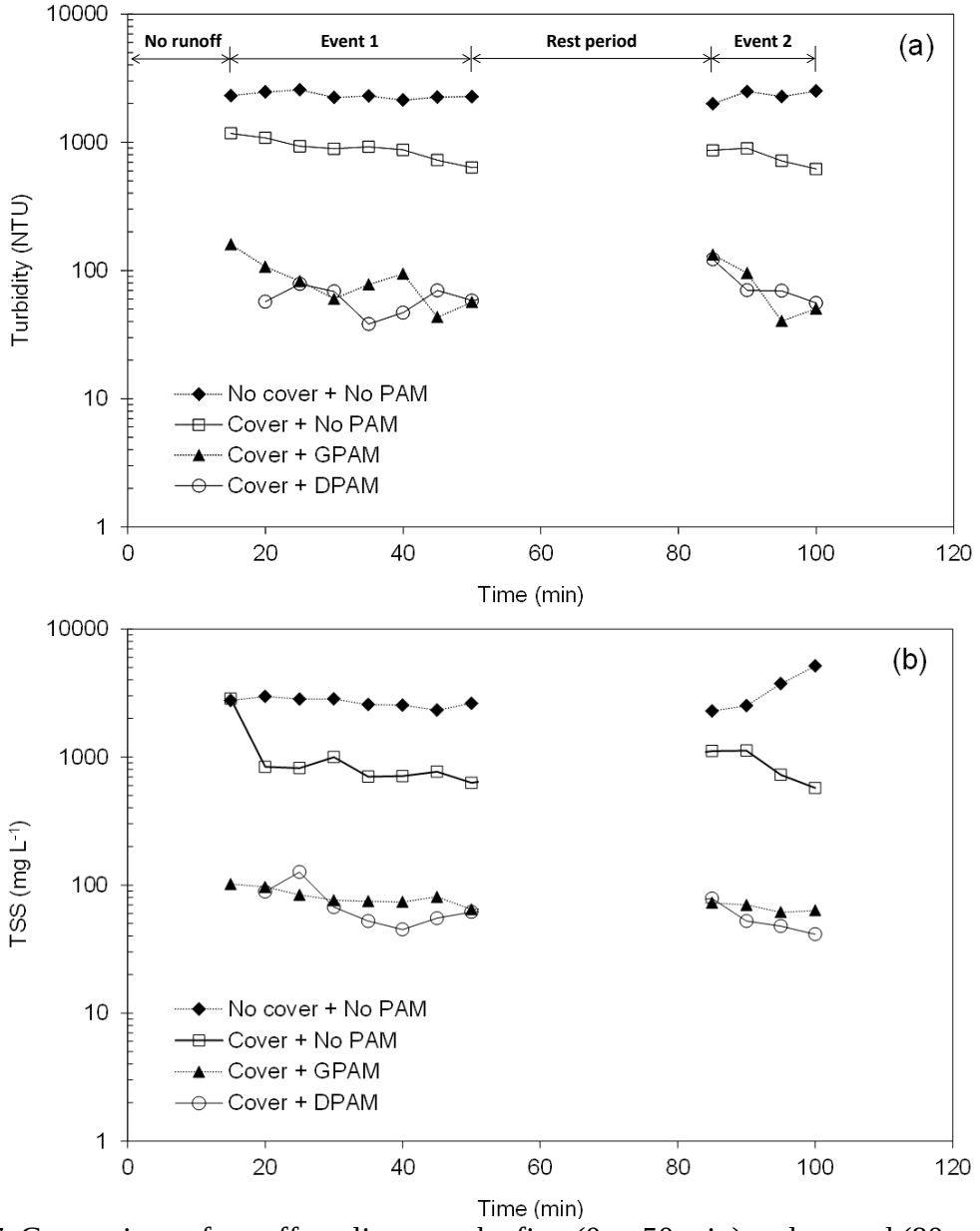

Figure 3.7. Comparison of runoff quality over the first (0 to 50 min) and second (80 to 100 min) rainfall events with a 30-min rest period between rainfall events for (a) turbidity and (b) total suspended solid (TSS) concentration. The GPAM and DPAM are granular and dissolved polyacrylamide (PAM), respectively. Note a logarithmic scale on y-axis.

The cover + DPAM treatment yielded the lowest erosion rate, which was attributable to both the lowest runoff rate and TSS, although TSS was not significantly different from cover + GPAM treatment (Table 3.4). The linear relationships between cumulative rainfall and cumulative sediment loss (Fig. 3.8) had clear separation in their slopes (kg ha^{-1} mm^{-1}): no cover + no PAM (278) > cover + no PAM > (117) > cover + GPAM (9.1) > cover + DPAM (4.4). These results suggest that the erosion rate for cover + DPAM was 63 times lower than bare soil and 26 times lower than the cover alone. The erosion rate for GPAM was more than twice that of DPAM with cover, which agrees with Babcock and McLaughlin (2013) who found better performance of DPAM over GPAM (applied with wheat straw) in reducing sediment loss.

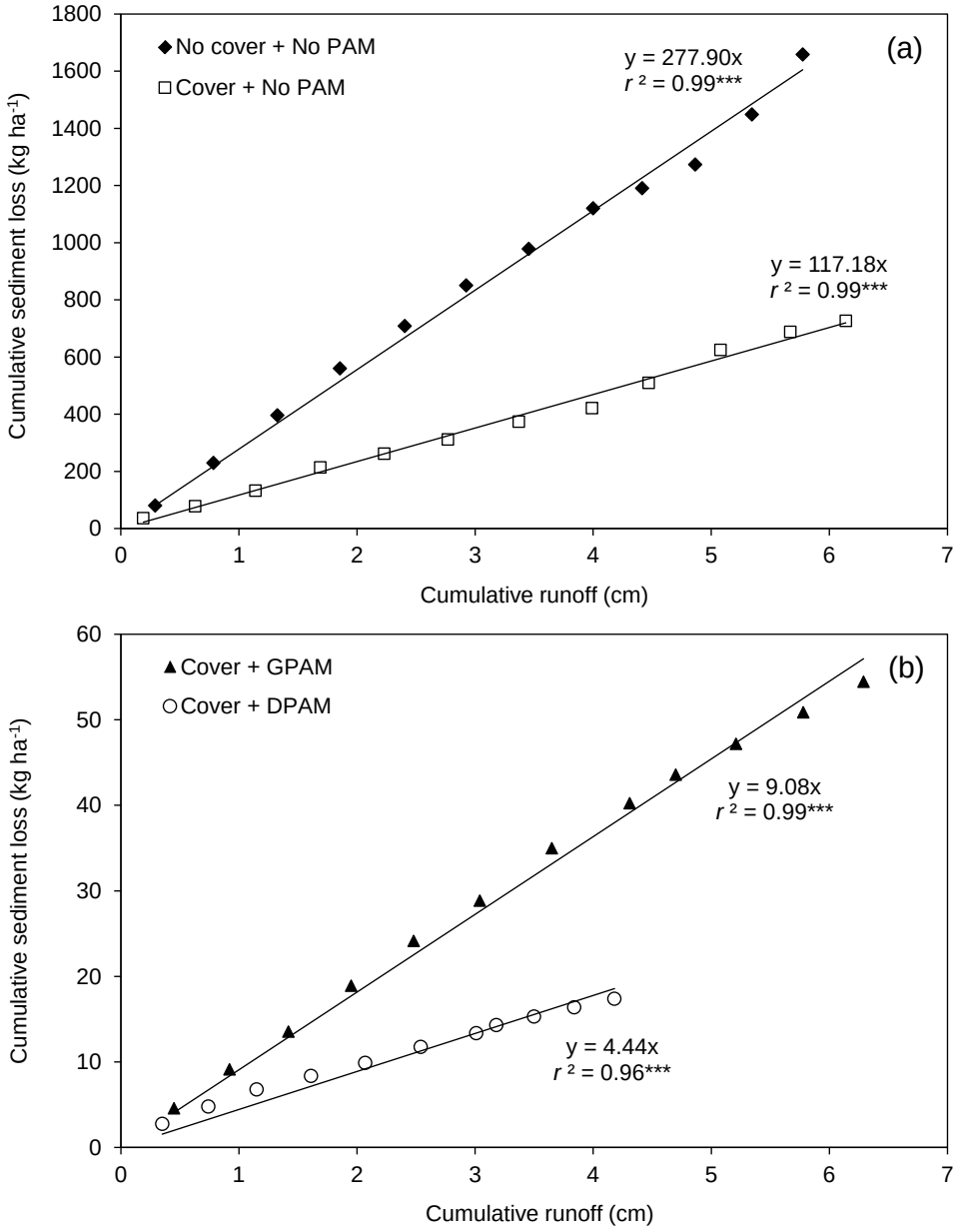

Figure 3.8. Cumulative sediment loss affected by polyacrylamide (PAM) treatment for (a) No PAM and (b) PAM. The GPAM and DPAM are granular and dissolved polyacrylamide (PAM), respectively.

3.2.3. Polyacrylamide loss

The concentration of PAM in runoff declined over time for both application methods (Fig. 3.9). PAM concentrations from the GPAM treatment were 13 to 17 mg L^{-1} in the first runoff samples of the first and second rain events, respectively, with declines to around 6 mg L^{-1} at the end. The PAM concentrations in the DPAM treatment were much lower at 4-5 mg L^{-1} initially, further dropping to < 1 mg L^{-1} by the end of the second event. Although the PAM loss was much smaller for DPAM than GPAM, both losses were relatively steady and were significantly related to the cumulative runoff amount (Fig. 3.10). Over the course of both rain events, the total losses of PAM in runoff for GPAM and DPAM were 19% and 2% of the applied amounts, respectively. Applied DPAM was likely to be more evenly distributed and with more complete contact with soil particles than GPAM (Seybold, 1994). We observed that the PAM granules sprinkled with water one day before rainfall simulation formed thin slimy patches in the applied area, somewhat similar to a "patch method" in furrow irrigation. The patch method is known to work well in most circumstances, but the PAM patch can be flushed out on steep slopes or high intensity rainfall events (Sojka et al., 2007; Babcock and McLaughlin, 2013). Overall, the DPAM treatment, which is similar to adding PAM granules to a hydroseeder tank during the filling and mixing processes, was superior in minimizing PAM loss compared to GPAM under our conditions. However, field studies with more typical natural rainfall intensities have not found significant differences between DPAM and GPAM performance (Babcock and McLaughlin, 2011).

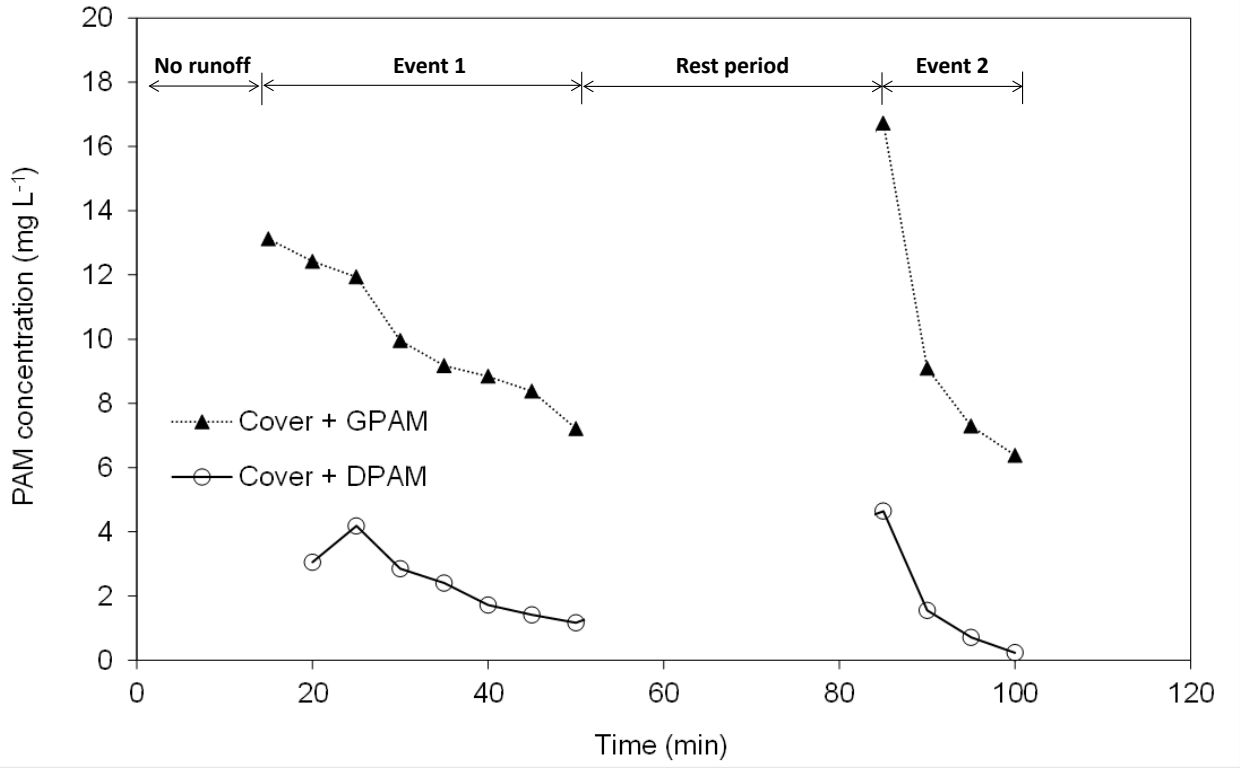

Figure 3.9. Polyacrylamide (PAM) concentration in runoff during the first (0 to 50 min) and second (80 to 100 min) rainfall events with a 30-min rest period between events. The GPAM and DPAM are granular and dissolved PAM, respectively.

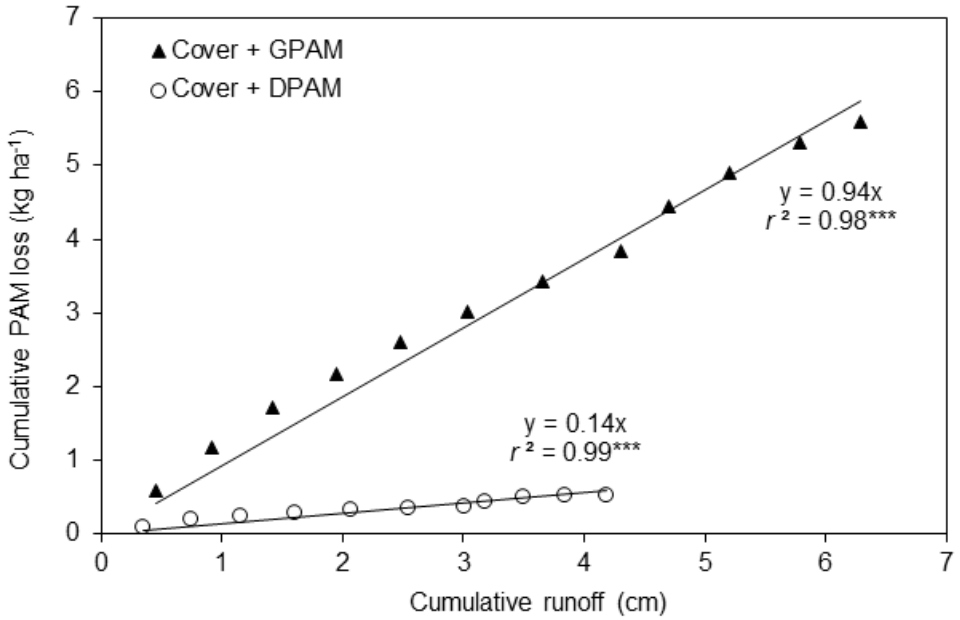

Figure 3.10. Granular and dissolved polyacrylamide (GPAM and DPAM, respectively) loss by runoff.

3.2.4. Particle size distribution in eroded sediments

The particle size distribution of eroded sediment was clearly affected by the cover and by PAM application (Table 3.5). The addition of a cover alone increased the mean particle size by 2-fold and the median diameter (D_{50}) by 3-fold. The application of PAM further increased mean particle sizes by more than 2.5- to 3-fold compared to the cover alone. Over the course of the rainfall simulations, the D_{50} was nearly constant in runoff from the bare soil, but fluctuated for the other treatments (data not shown). We presume that with the high erosion rate in the bare soil treatment, fresh soil was being continually exposed during the rainfall simulation, so the particle size distribution remained constant. The increase in particle size with the sediment being lost would be beneficial in trapping or settling the eroded sediment when appropriate sediment control practices are in place (Haan et al., 1994).

Table 3.5. Summary of particle size (mean ± std. error) averaged over time in eroded sediments.

Particle size[a]	No cover + No PAM	Cover + No PAM	Cover + GPAM	Cover + DPAM
	---------- µm ----------			
Mean	24 ± 1.4	50 ± 5.0	161 ± 8.9	137 ± 21
D_{10}	1.4 ± 0.1	6.1 ± 0.7	18 ± 2.2	11 ± 1.8
D_{50}	12 ± 0.3	38 ± 3.0	117 ± 8.8	85 ± 14
D_{90}	60 ± 5.8	108 ± 81	375 ± 26	337 ± 56

[a] D_{10}, D_{50}, and D_{90} are particle diameters corresponding 10^{th}, 50^{th}, and 90^{th} percentile, respectively.

Smaller particle sizes in the runoff sediments from control treatment pose turbidity issues because conventional gravity-based sediment control practices are not effective in trapping fine sediments due to their low settling velocity (Line and White, 2001; Pitt et al, 2007; McCaleb and

McLaughlin, 2008). There was a clear relationship between particle size (D_{50}) and turbidity in the runoff samples with an exponential decrease in turbidity with increasing D_{50} (Fig. 3.11). Runoff from control treatment had populated D_{50} values in finer size range (<15 µm), which contributed the most to turbidity. Runoff from GPAM or DPAM treatment contained agglomerated sediments as a result of flocculation between PAM molecules and soil particles, having much lower turbidity range (<200 NTU) regardless of their corresponding D_{50} values.

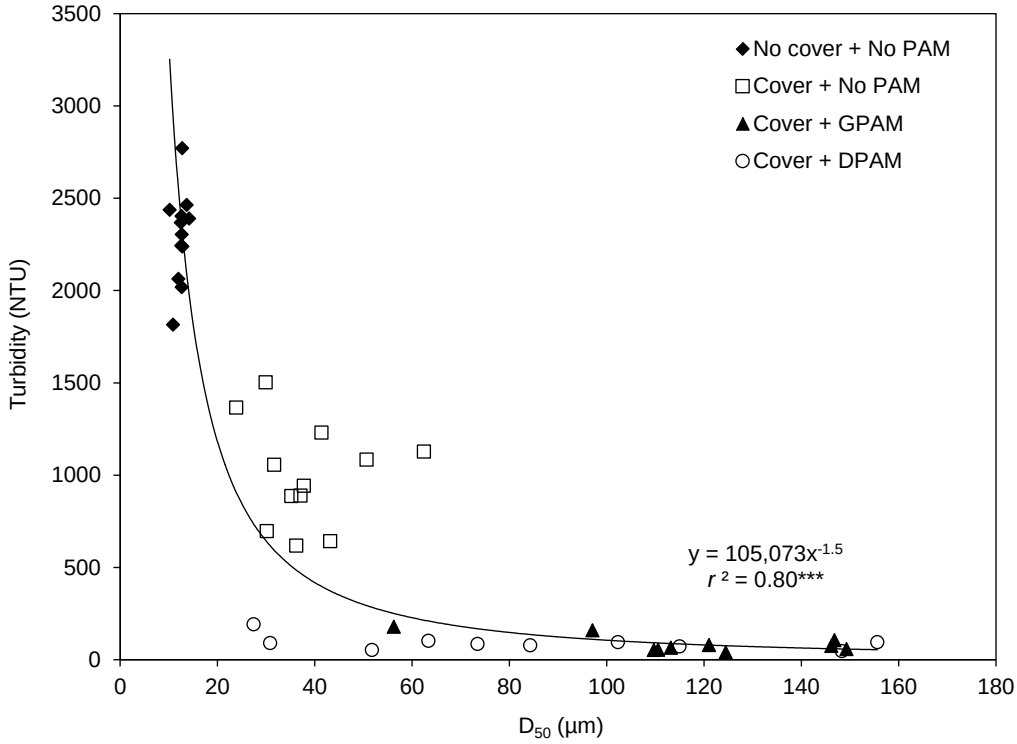

Figure 3.11. Turbidity as a function of median particle diameter (D_{50}) in eroded sediments.

3.2.5. Summary

With increasing regulation of construction site stormwater runoff, use of PAM is becoming a widespread best management practice for erosion and turbidity control. However, major uncertainties exist about the optimal application techniques to meet both water quality goals and environmental safety of applied PAM products. Our results demonstrated that excelsior ECB with granular or dissolved PAM (GPAM and DPAM, respectively) applications greatly improved runoff water quality under simulated rainfall. In addition, sediment from both PAM treatments had increased particle sizes compared to untreated sediments, suggesting an enhanced settling potential of the flocculated runoff sediment.

Our study suggests that the method of PAM application for erosion control may be a significant factor in PAM losses by runoff. The DPAM applied in concentrated solution (500 mg L^{-1}) yielded much lower PAM concentration in runoff (1.3 mg L^{-1} in flow-weighted conc.) than GPAM (8.9 mg L^{-1}) under intense rainfall simulation. These PAM concentrations, particularly with DPAM, are still far below levels considered to be toxic to aquatic organisms (>100 mg L^{-1}). In contrast, the turbidity levels in untreated runoff are likely to be far above known toxicity levels for aquatic organisms (Henley et al., 2000).

3.3. Column Experiment

3.3.1. Hydraulic conductivity

Dissolved PAM applied in two different application modes, pulse and continuous step input respectively, reduced the HC in the receiving columns (Fig. 3.12). Prior to PAM addition, the HC of the study soil was 4 cm h^{-1}, but it was reduced by a 100-fold under the pulse input and 10,000-fold under the step input. The pulse input applied with 500 mg L^{-1} of dissolved PAM in a small volume (0.6 PV) reduced the HC rapidly within 5 PV and the values of HC remained to be the same after the water source was switched to the DI water. The step input applied with 25 mg L^{-1} of dissolved PAM reduced the HC in a greater extent (< 0.001 cm h^{-1}) than the pulse input (< 0.1 cm h^{-1}) and its HC values further decreased with continuous addition of the PAM solution.

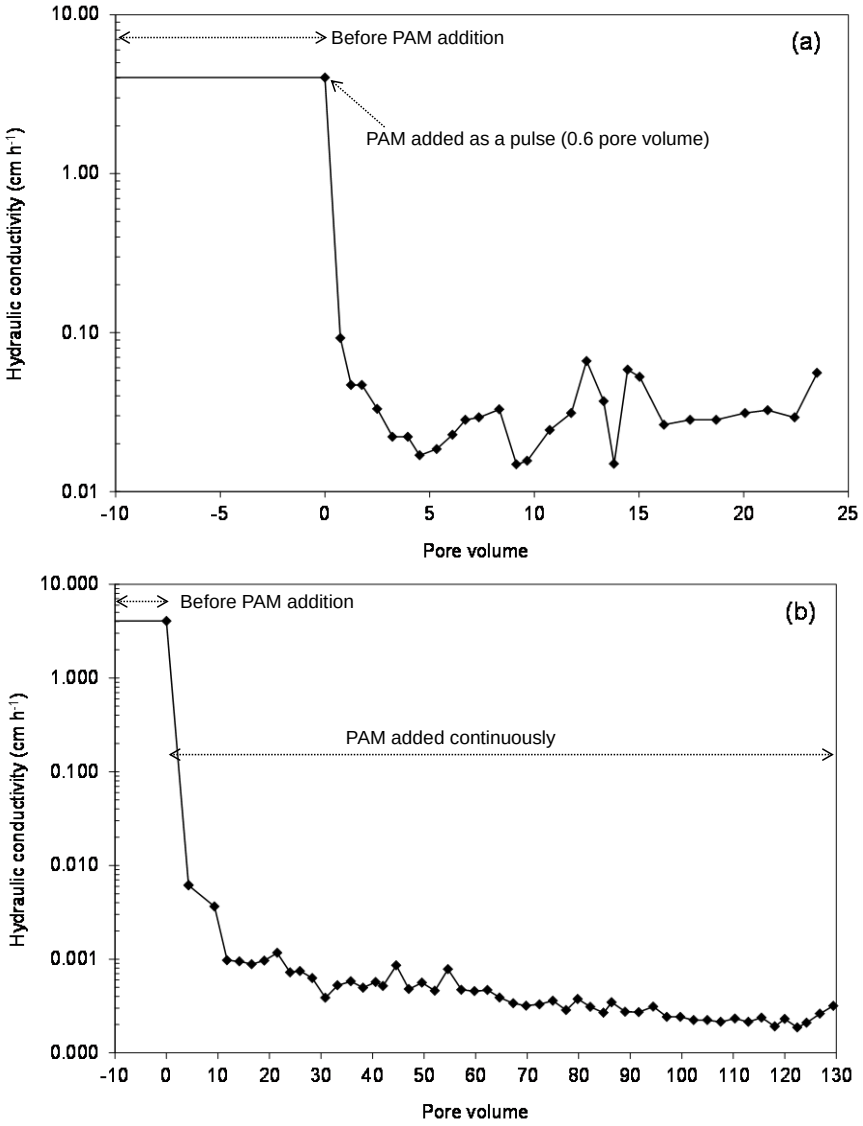

Figure 3.12. The hydraulic conductivity of the Piedmont clay loam applied with (a) pulse input of PAM solution (500 mg L^{-1}) and (b) step input of PAM solution (25 mg L^{-1}). Note a logarithmic scale on Y-axis.

Infiltration rate and hydraulic conductivity can either increase or decrease depending on the type and concentration of PAM applied, soil properties, and application protocol. Infiltration decreases have been found with increasing charge density of polymer material, which was attributable to increased viscosity associated with higher charge density (Malik and Letey, 1992; Falatah et al., 1999). The PAM materials (A150) tested in this study was a high-molecular weight with 50 % anionic charge density, which was likely to block soil pores rapidly in both application modes. Our results are in agreement with previous studies (Ajwa and Trout, 2006; Lentz, 2008) in that infiltration decreased in the PAM-treated soils when concentrated PAM (>125 mg L^{-1}) was applied or continuously applied at low concentration (5-20 mg L^{-1}). Increased filtration rates after PAM addition have been only found when the soils were pretreated with PAM solutions at low concentration (5-20 mg L^{-1}) and allowed to dry before irrigation in medium-textured soils (Ajwa and Trout, 2006; Sojka et al., 2007; Shainberg et al., 2011). In this case, the cohesive properties of PAM may bind soil particles and peds together, keeping open larger soil pores through which water preferentially flows and this condition would be relevant to irrigation furrows on agricultural fields where soil management would encourage such structure (Sojka et al., 2007).

The value of HC depends on both the soil pore size distribution of the soil and the viscosity of the water (Letey, 1996). There is a proportional inverse relationship between HC and viscosity. In this study, the viscous PAM solution was likely to move preferentially toward greater pore sizes. Sojka et al. (2007) noted that PAM infiltration effects are a balance between prevention of surface sealing and apparent viscosity increases in soil pores. If there is a lack of aggregation (e.g., sandy soil), PAM's tendency to increase viscosity of the infiltrating water becomes the dominant phenomenon due to the limited influence of soil structure on sealing under these conditions. Column infiltration study by Ajwa and Trout (2006) confirmed that the fluid properties of PAM solutions increased resistance of flow rather than preserving aggregate structure, which resulted in reduced infiltration in sandy loam soil.

3.3.2. PAM displacement

Leaching of dissolved PAM through 2-cm repacked column was strongly retarded by the soil material. In the pulse input, PAM began to elute at 2 PV and stopped its elution after 17 PV (Fig. 3.13). In the step input, PAM began to elute at 12 PV and there was continuous elution of PAM with the continuing PAM throughput (128 PV) at 25 mg L^{-1}. The higher source strength of PAM (500 mg L^{-1}) in the pulse input was likely to result in relatively early elution compared to step input. Later elution in the step input indicates that there was more reaction (i.e., adsorption) initially between soil material and PAM molecules. Relative amount of PAM leached against total amount of PAM was 14 % for the pulse input with 23 PV water throughput and 23 % for the step input with 128 PV. It was notable that the step input up to 128 PV did not allow complete displacement of PAM (i.e., 100 % of PAM leached). This result is in agreement with Sojka et al. (2007) who noted that penetration of high molecular weight PAMs is limited to a few centimeters from the soil surface due to the length of the polymer chain and large number of adsorption sites along the PAM molecule.

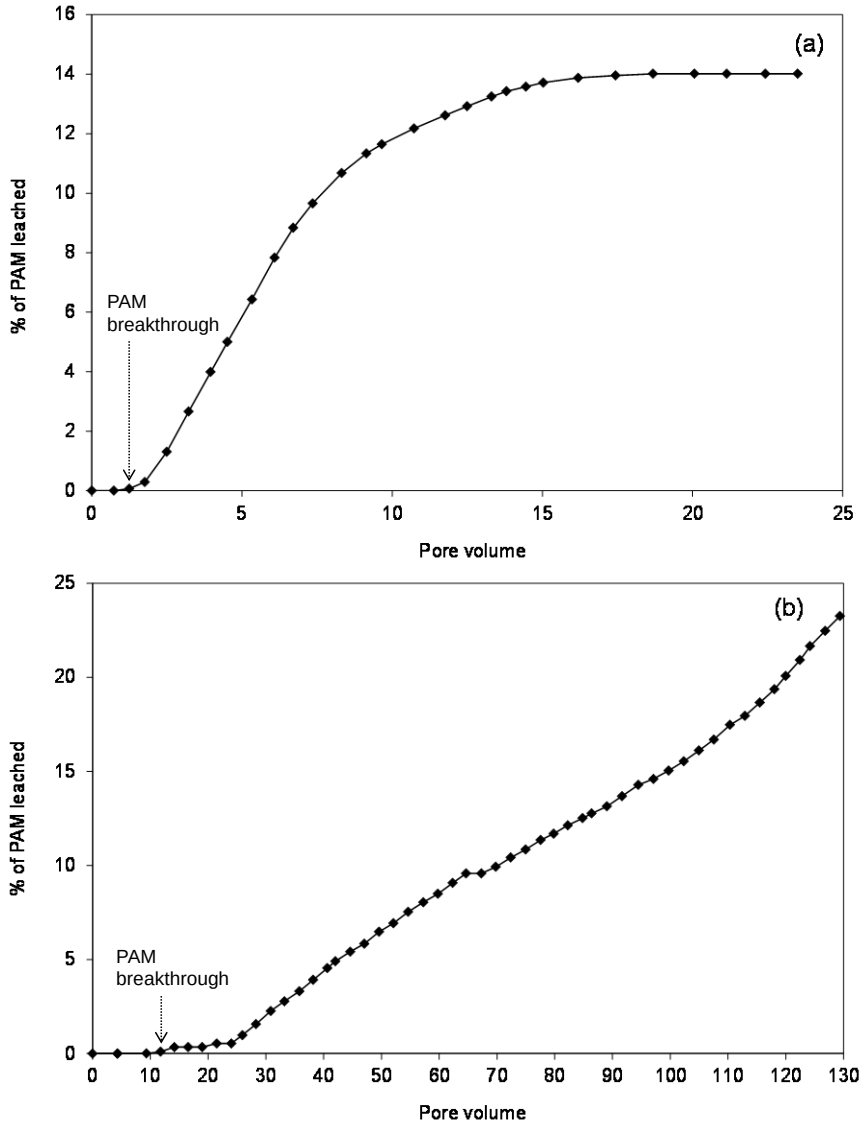

Figure 3.13. Mass fraction (%) of the cumulative amount of polyacrylamide (PAM) leached relative to the cumulative amount of PAM applied: (a) pulse input of PAM solution (500 mg L^{-1} at 30 kg ha^{-1}) and (b) step input of PAM solution (25 mg L^{-1} at a total rate of 319 kg ha^{-1}).

3.3.3. PAM transport and CXTFIT modeling

Data from PAM breakthrough curve (i.e., C/C_o as a function of pore volume, PV) were best-fitted by two-region physical non-equilibrium model in the CXTFIT (Fig. 3.14). Both equilibrium and chemical non-equilibrium models were poorly fitted (data not shown). With the pulse input, the highest relative concentration was only 0.012 at the PV range between 4 and 8, and its breakthrough curve had a long-tailing, indicating a strong interaction between PAM and soil. With the step input, the relative concentrations in leachate initially increased up to 0.35 but bounced up and down afterward, resulting in a relatively low coefficient of determination of the fitted curve ($R^2 = 0.50$) compared to that of the step input ($R^2 = 0.97$). These results in addition to the decreases in the HC may be associated with the way PAM molecules are adsorbed in the soil and subsequent influences on available pore spaces as conduits for the large PAM molecules. Malik and Letey (1996) postulated that as one segment of PAM molecules is adsorbed in soil

surface, other sections may extend away from the surface into the pore and thus create drag on the flowing water. In other words, the large PAM molecules become deformed to “squeeze” through the pore necks. These phenomenons were likely to reason for the best fitting model found with two-region physical non-equilibrium model that considers two distinct mobile (flowing) and immobile (stagnant) liquid regions in the soil pores.

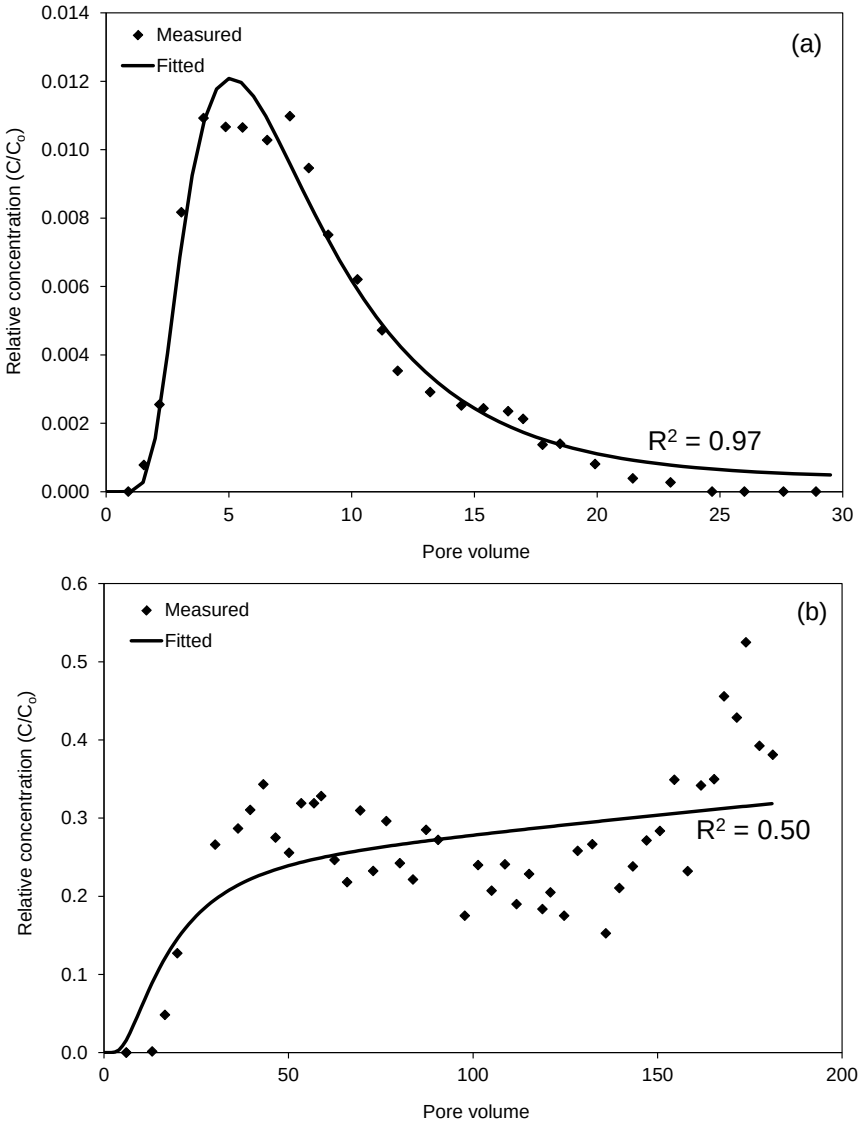

Figure 3.14. Breakthrough curve of polyacrylamide (PAM) in a 2-cm long column applied with (a) pulse input of PAM solution (500 mg L^{-1}) and (b) step input of PAM solution (25 mg L^{-1}).

Retardation factor, which is defined as the number of PV at which the relative concentration of the measured BTC is 0.5, was estimated to be >2300 in both pulse and step input conditions of PAM (Table 3.6). This suggested a strong retardation of dissolved PAM into the soil material regardless of the PAM application modes. The mobile water fraction (β) ranged from 0.02 to 0.07, indicating limited pore spaces available for the large PAM molecule to flow through. This may cause larger immobile domain and more chemical reaction between mobile and immobile

phases. The ω values determined by CXTFIT were low, indicating that diffusive mass transfer between mobile and immobile phases was slow.

Table 3.6. PAM transport parameters obtained from the CXTFIT simulations.

PAM application mode	CXTFIT output			
	R	D_m	β	ω
		$cm^2\ h^{-1}$		
Pulse	2321	2.06	0.02	0.008
Step	2373	1.57	0.07	0.027

R = retardation factor; D_m = dispersion coefficient of mobile phase; β = mobile water fraction; ω = mass transfer coefficient between mobile and immobile phases.

3.3.4. PAM sorption isotherm

Batch PAM sorption data for the range of concentrations of interest (≤ 100 mg L^{-1}) were fitted well by the Langmuir model with an r^2 of 0.99 (Fig. 3.15). Previous researches have shown similar L-shaped PAM sorption in kaolinte (Nabzar et al., 1984), morillonite (Ben-Hur et al., 1992), and organic-matter removed soils (Lu et al., 2002). The linearized Langmuir yielded 1,353 mg kg^{-1} for S_{max} and 1.31 L mg^{-1} for K_L. The initial PAM concentraton at 25 mg L^{-1} became 0.5 mg L^{-1} after the 24-h equilibration and the R value at 0.5 mg L^{-1} (i.e., slope in the isotherm curve) was estimated to be 2,061, which was close to that from the column experiment.

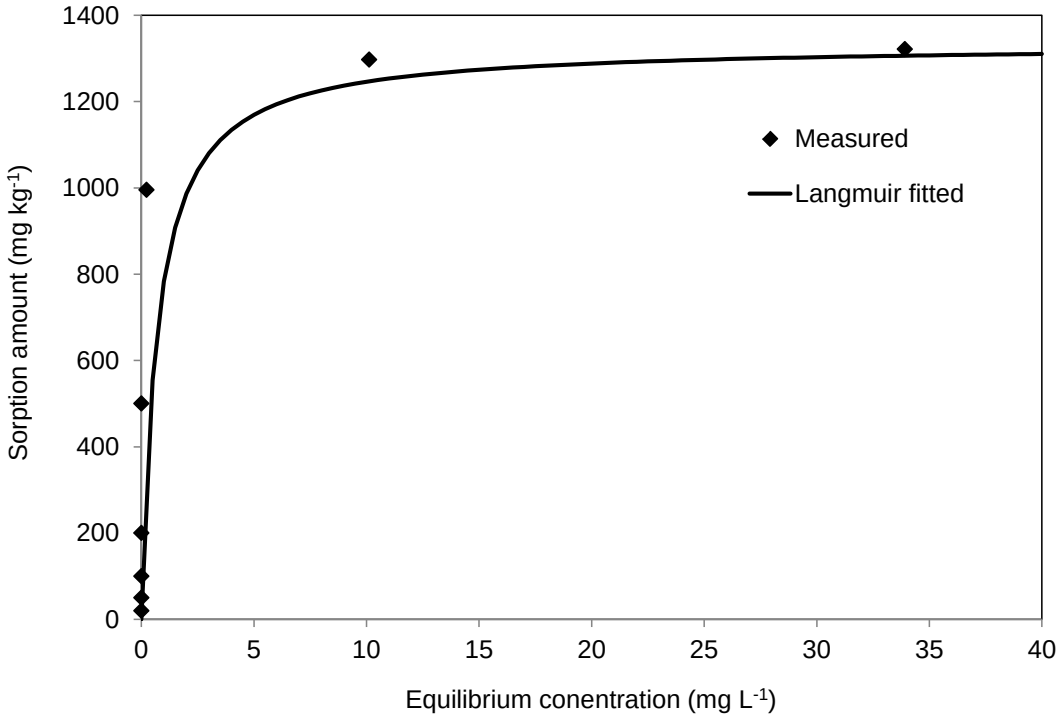

Figure 3.15. Polyacrylamide sorption isotherm for the study soil material and a model fit using Langmuir equation.

3.3.5. Summary

Our study demonstrated that PAM application under saturated condition without a drying period could greatly reduce the HC in the 2-cm repacked sandy clay loam soil. The reduction of HC was greater with the step input of PAM solution. Leaching of applied PAM solution was strongly limited as the soil material acted as a strong sorbent for the PAM molecules. The interaction between the viscous PAM molecules and soil under saturated condition favored the potential use of the PAM toward seepage-inhibiting sealants. The CXTFIT results suggested that dual porosity model (two physical-regions, mobile and immobile) was the best fit for our observed data and physical non-equilibrium was established once the PAM solution was applied to the surface soil under saturated condition.

4.0 Conclusions and Recommendations

Previous studies have clearly indicated the potential benefits of using PAM for erosion and sediment control. This study confirms the benefits and provides further information on the details of how PAM behaves when applied to soil. The following is a summary of each part of the study and the implications of the results:

1) The hyamine test can be used to detect PAM in clear water to < 1 mg L^{-1}, several orders of magnitude below typical levels of concern. In water extracted with soil materials, the detection limit ranges from 0.3-22 mg L^{-1} depending on the soil and PAM properties, with higher values with lower PAM charge densities. Sediment sources with organic carbon content >0.5% produce interferences which make this method impractical for PAM detection. If PAM concentrations in runoff water are desired, each site would have to have a response curve developed specific to that site. The method is relatively inexpensive and uses simple turbidity meters commonly found in water testing operations.

2) The rainfall simulation tests supported previous work indicating that the addition of PAM to a groundcover significantly reduces erosion and turbidity in runoff water. Under the relatively heavy rainfall simulation, dissolved PAM was slightly more effective since it was fully activated and reactive. Peak PAM concentrations in runoff were higher with granular applications (13-17 mg L^{-1}) compared to dissolved (4-5 mg L^{-1}), with resulting total losses of 19% and 2% of applied, respectively. This suggests that dissolved PAM is preferred over granular PAM for erosion control, but the application of either is highly beneficial in reducing erosion and improving runoff water quality as vegetation is being established. The concentrations of PAM in runoff are below levels of concern for environmental exposures.

3) The application of PAM increased the size of particles eroded from the test boxes by a factor of 2-3X. The larger particle size would greatly enhance settling behind typical practices on construction sites, such as silt fences and sediment basins.

4) PAM greatly reduced infiltration when applied either as a concentrated solution (similar to a hydroseeding use) once or as a more dilute solution constantly, when applied to a saturated soil. However, other studies have shown that if the soil is allowed to dry, this effect is reversed.

5) For the concentrated solution, PAM was detected after 2 pore volumes of water passed through the 2 cm of soil in the columns, but only 14% of the PAM leached through the column after more than 25 pore volumes. For the dilute solution, more than 10 pore volumes were needed for PAM to pass through the 2 cm of soil, and only after 25 pore volumes did the PAM

breakthrough reach a steady state. This demonstrates that PAM is not likely to leach far in soil under typical conditions and tends to react to the soil surfaces as it passes through.

References

Aase, J. K., Bjorneberg, D. L., and Sojka, R. E. (1998). Sprinkler irrigation runoff and erosion control with polyacrylamide-laboratory tests. Soil Sci. Soc. Am. J. 62, 1681–1687.

Agrawal, Y.C., I.N. McCave, and J.B. Riley. 1991. Laser diffraction size analysis. In: Syvitski, J.P.M.(ed) Principle, method, and application of particle size analysis. Cambridge University Press, pp 119-128.

Akhtar, M.S., Richards, B.K., Medrano, P.A., DeGroot, M., Steenhuis, T.S., 2003. Dissolved phosphorus from undisturbed soil cores: related to adsorption strength, flow rate of soil structure? Soil Sci. Soc. Am. J. 67 (2), 458–470.

Allison, J.D., J.W. Wimberly, and T.L. Ely. 1987. Automated and manual methods for the determination of polyacrylamide and other anionic polymers. Spe. Reserv. Eng. 2:184–188.

Armbruster, D.A., and T. Pry. 2008. Limit of blank, limit of detection and limit of quantification. Clin. Biochem. Rev 29(Suppl 1): S49–S52.

Babcock, D.L., and R.A. McLaughlin. 2011. Runoff water quality and vegetative establishment for groundcovers on steep slopes. J. Soil Water Conserv. 66:132-141.

Babcock, D.L., and R.A. McLaughlin. 2013. Erosion control effectiveness of straw, hydromulch, and polyacrylamide in a rainfall simulator. J. Soil Water Cons. 68:221-227.

Barvenik, F.W. 1994. Polyacrylamide characteristics related to soil applications. Soil Sci. 158:235-243.

Ben-Hur, M., and J. Letey. 1989. Effect of polysaccharides, clay dispersion, and impact energy on water infiltration. Soil Sci. Soc. Am. J. 53:233-238.

Ben-Hur, M., M. Malik, J. Letey, and U. Mingelgrin. 1992. Adsorption of polymers on clays as affected by clay charge and structure, polymer properties, and water quality. Soil Sci. 153:349-356.

Bhardwaj, A. K., R.A. McLaughlin, I. Shainberg, and G.J. Levy. 2009. Hydraulic characteristics of depositional seals as affected by exchangeable cations, clay mineralogy, and polyacruylamide. Soil Sci. Soc. Am. J. 73:910-918.

Bureau of Census. 2010. State population rankings summary. U.S. Bureau of the Census, http://www.census.gov/population/projections/state/9525rank/ncprsrel.txt (Accessed on 7/16/2010).

Clesceri, L.S., A.E. Greenberg, and A.D. Eaton. 1998. Standard Methods for the Examination of Water and Wastewater, 20th ed. Washington DC: APHA, AWWA, WEF.

Crummett, W.B., and A. Hummel. 1963. The determination of traces of polyacrylamides in water. J. Am. Water Works Assoc. 55:209-219.

Entry, J.A., R.E. Sojka, and B.J. Hicks. 2008. Carbon and nitrogen stable isotope ratios measurement of anionic polyacrylamide degradation in soil. Geoderma. 145:8-16.

Erhart, B. J., R. D. Shannon, and A. R. Jarrett. 2002. Effects of construction site sedimentation basins on receiving stream ecosystems. Trans. Am Soc. Agric. and Bio. Eng. 45: 675-680.

Eshel, G., G.J. Levy, U. Mingelgrin, and M.J. Singer. 2004. Critical evaluation of the use of laser diffraction for particle-size distribution analysis. Soil Sci. Soc. Am. J. 68(3): 736-743.

Falatah, A. M., A. M. Al-Omran, A. A. Shalaby, and M. M. Mursi. 1999. Infiltration in a calcareous sandy soil as affected by water-soluble polymers. Arid Soil Res. Rehabil. 13:61-73.

Fetter, C.W., 1999. Contaminant Hydrogeology, 2nd ed. Prentice Hall, Upper Saddle River, NJ.

Flanagan, D. C., K. Chaudhari, and L. D. Norton. 2002a. Polyacrylamide soil amendment effects on runoff and sediment yield on steep slopes. Part 1. Simulated rainfall conditions. Trans. ASABE. 45: 1327-1337.

Flanagan, D. C., K. Chaudhari, and L. D. Norton. 2002b. Polyacrylamide soil amendment effects on runoff and sediment yield on steep slopes. Part 2. Natural rainfall conditions. Trans. ASABE. 45: 1339-1351.

Flanagan, D.C., K. Chaudhari, and L.D. Norton. 2002a. Polyacrylamide soil amendment effects on runoff and sediment yield on steep slopes: Part I. Simulated Rainfall Conditions. Trans. ASABE. 45:1327-1337.

Flanagan, D.C., K. Chaudhari, and L.D. Norton. 2002b. Polyacrylamide soil amendment effects on runoff and sediment yield on steep slopes: Part II. Natural Rainfall Conditions. Trans. ASABE. 45:1339-1351.

Haan, C.T., B.J. Barfield, and J.C. Hayes. 1994. Design hydrology and sedimentology for small catchments. Academic Press Inc., San Diego, CA.

Harris, D.C. 2007. Quantitative chemical analysis. 7th ed. W. H. Freeman and Company, New York.

Hayes, S. A., R.A. McLaughlin, and D.L. Osmond, 2005. Polyacrylamide Use for Erosion and Turbidity Control on Construction Sites, J. Soil and Water Conserv. 60(4):193-199.

Helalia, A.M., and J. Letey. 1988. Cationic polymer effects on infiltration with a rainfall simulator. Soil Sci. Soc. Am. J. 52:247-250.

Henley, W.F., M.A. Patterson, R.J. Neves, and A.D. Lemly. 2000. Effects of sedimentation and turbidity on lotic food webs: a concise review for natural resource managers. Rev. Fish. Sci. 8:125-139.

Herbert Jr., R.B. 2011. Implications of non-equilibrium transport in heterogeneous reactive barrier systems: Evidence from laboratory denitrification experiments. J. Contam. Hydrol. 123:30-39.

Hillel, D. 2004. Introduction to Soil Physics. Elsevier - Academic Press, San Diego, CA.

Hunt, J.A., T.S. Young, D.W. Green, and G.P. Willhite. 1988. Size-exclusion chromatography in the measurement of concentration and molecular weight of some EOR polymers. Spe. Reserv. Eng. 3:835-841.

Husein A. A., and T. J. Trout. 2006. Polyacrylamide and water quality effects on infiltration in sandy loam soils. Soil Sci. Soc. Am. J. 70:643-650.

Jungreis, E. 1981. A simple microdetermination of polymer flocculants (polyacrylamides and guar) in mine water. Analyt. Lett. 14:1177-1183.

Kang J., T.D. Sowers, O.W. Duckworth, A. Amoozegar, J.L. Heitman, and R.A. McLaughlin. 2013a. Turbidimetric determination of anionic polyacrylamide in low carbon soil extracts. J. Environ. Qual. 42:1902-1907.

Kang, J., M.M. McCaleb, and R.A. McLaughlin. 2013b. Check dam and polyacrylamide performance under simulated stormwater flow. J. Environ. Manage. 129:593-598.

Klute, A. (ed.) 1986. Methods of Soil Analysis, Part 1. Physical and Mineralogical Methods. Agronomy Monograph (2nd ed.). Am. Soc. of Agro., Madison, WI.

Kuss, H. J. 2003. Weighted least-squares regression in practice: selection of the weighting exponent. LC GC Europe, 16(12):819-823.
Lal, R., and A. Shukla. 2004. Principles of soil physics. Marcel Dekker, Inc., New York.
Lentz, R. D. 2008. Inhibiting water infiltration with polyacrylamide and surfactants: Applications for irrigated agriculture. J. Soil Water Conserv. 58:290-299.
Lentz, R. D., and R. E. Sojka. 2009. Long-term polyacrylamide formulation effects on soil erosion, water infiltration, and yields of furrow-irrigated crops. Agron. J. 101: 305-314.
Lentz, R. D., R. E. Sojka, and J. A. Foerster. Estimating polyacrylamide concentration in irrigation water. 1996. J. Environ. Qual. 25:1015-1024
Letey, J. 1996. Effective viscosity of PAM solutions through porous media. In Proceedings of the managing irrigation-induced erosion and infiltration with polyacrylamide (R. E. Sojka and R. D. Lentz, Eds). May 6-8, 1996, College of Southern Idaho, Twin Falls, ID. University of Idaho Misc. Pub. 101-96, pp 94-96.
Levy, G.J., J. Levin, M. Gal, M. Ben-Hur, and I. Shainberg. 1992. Polymers' effects on infiltration and soil erosion during consecutive simulated sprinkler irrigations. Soil Sci. Soc. Am. J. 56: 902-907.
Line, D.E., and N.M. White. 2001. Efficiencies of temporary sediment traps on two North Carolina construction sites. Trans. ASABE. 44:1207-1215.
Lu, J. H., L. Wu, and J. Letey. 2002. Effects of soil and water properties on anionic polyacrylamide sorption. Soil Sci. Soc. Am. J. 66:578-584.
Lu, J., and L. Wu. 2003b. Polyacrylamide distribution in columns of organic matter-removed soils following surface application. J. Environ. Qual. 32:674-680.
Lu, J., and L. Wu. 2003a. Polyacrylamide quantification methods in soil conservation studies. J. Soil Water Conserv. 58:270-275.
Lu, J.H., and L. Wu. 2001. Spectrophotometric determination of polyacrylamide in waters containing dissolved organic matter. J. Agr. Food Chem. 49:4177-4182.
Malik, M., and J. Letey. 1992. Pore-size dependent apparent viscosity for organic solutes in saturated porous media. Soil Sci. Soc. Am. J. 56: 1032-1035.
McCaleb, M.M., and R.A. McLaughlin. 2008. Sediment trapping by five different sediment detention devices on construction sites. Trans. ASABE. 51: 1613-1621.
McLaughlin, R. A. and T. T. Brown. 2006. Performance of erosion control materials and polyacrylamide under field and rainfall simulator conditions. J. Am. Water Resour. As. 42(3):675-684.
McLaughlin, R. A., S. A. Hayes, D. L. Clinton, M. S. McCaleb, and G. D. Jennings. 2009. Water quality improvements using modified sediment control systems on construction sites. Trans. ASABE 52: 1859-1867.
McLaughlin, R.A. and N. Bartholomew. 2007. Effects of polyacrylamide and soil properties on flocculation. Soil Sci. Soc. Am. J. 71:537-544.
Michaels, A.S., and O. Morelos. 1955. Polyelectrolyte adsorption by kaolinite. Ind. Eng. Chem. 47:481-488.
Moreau, D. 1992. Declining rates of expansion of reservoir capacity in North Carolina / by David H. Moreau. *Report ; no. 272* [Raleigh] : Water Resources Research Institute of the University of North Carolina.
Nabzar, L., E. Pefferkorn, E., and R. Varoqui. 1984. Polyacrylamide-sodium kaolinite interactions: Flocculation behavior of polymer clay suspensions. J. Colloid Interface Sci. 102:380-388.

NCDENR. 2006. Erosion and Sediment Control Design Manual, Chapter 8, Appendices. Raleigh, NC: North Carolina Department of Environment and Natural Resources. Available at http://portal.ncdenr.org/web/lr/publications. Assessed on Oct 18, 2013.
Novotny, V., and H. Olem. 1994. Water quality: prevention, identification and management of diffuse pollution. Van Nostrand Reinhold, New York, New York, USA.
Peterson, J.R., D.C. Flanagan, and J.K. Tishmack. 2002. PAM application method and electrolyte source effects on plot-scale runoff and erosion. Trans. ASABE. 45:1859-1867.
Pitt, R., S.E. Clark, and D. Lake. 2007. Construction Site Erosion and Sediment Controls. DESTech Publications, Lancaster, PA.
Rudén, C. 2004. Acrylamide and cancer risk - expert risk assessments and the public debate. Food Chem. Toxicol. 42:335–349.
SAS. 2011. SAS/STAT® 9.3 User's Guide: The ANOVA procedure. Cary, NC: SAS Institute Inc.
Scoggins, M.W., and J.W. Miller. 1979. Determination of water-soluble polymers containing primary amide groups using the starch-triiodide method. Soc. Petrol. Eng. J. 19:151-154.
Seybold, C.A. 1994. Polyacrylamide review: soil conditioning and environmental fate. Commun. Soil Sci. Plant Anal. 25:2171-2185.
Shainberg, I., D. Goldstein, A.I. Mamedov, and G.J. Levy. 2011. Granular and dissolved polyacrylamide effects on hydraulic conductivity of a fine sand and a silt loam. Soil Sci. Soc. Am. J. 75:1090-1098.
Sirjacobs, D., I. Shainberg, I. Rapp, and G. J. Levy. 2000. Polyacrylamide sediments, and interrupted flow effects of rill erosion and intake rate. Soil Sci. Soc. Am. J. 64:1487-1495.
Smith-Palmer, T., B.R. Wentzell, J.C. Donini, and R.J. Jerrard. 1988. A tensammetric study of polyacrylamides including their determination. Can. J. Chem. 66:2658-2663.
Sojka, R. E., D. L. Bjorneberg, J. A. Entry, R. D. Lentz, and W. J. Orts. 2007. Polyacrylamide in agriculture and environmental land management. Adv. Agron. 92:75-162.
Sojka, R. E., R. D. Lentz, and D. T. Westermann. 1998. Water and erosion management with multiple applications of polyacrylamide in furrow irrigation. Soil Sci. Soc. Am. J. 62, 1672–1680.
Sojka, R.E., D.L. Bjorneberg, J.A. Entry, R.D. Lentz, and W.J. Orts. 2007. Polyacrylamide in agriculture and environmental land management. Adv. Agron. 92:75–162.
Soupir, M.L., S.A. Mostaghimi, A. Masters, K.A. Flahive, D.H. Vaughan, A. Mendez, and P.W. McClellan. 2004. Effectiveness of polyacrylamide (PAM) in improving runoff water quality from construction sites. J. Am. Water Resour. As. 40:53-66.
Southern Rural Development Center. 2010. http://srdc.msstate.edu/data/center/ncarolina.html (Accessed on 9/13/2010)
Taylor, K.C, and H.A. Nasr-El-Din. 1994. Acrylamide copolymers: A review of methods for the determination of concentration and degree of hydrolysis. J. Petrol. Sci. Eng. 12:9–23.
Toride, N., F.J. Leij, and M.Th. van Genuchten. 1999. *The CXTFIT code for estimating transport parameters from laboratory or field tracer experiments. Version 2.1*. Res. Rep. 137. Riverside, CA: U.S. Salinity Laboratory, USDA-ARS.
Toride, N., Leij, F. J., van Genuchten, M. Th., 1999. The CXTFIT code for estimating transport parameters from laboratory or field tracer experiments. Version 2.1. Res. Rep. 137. U.S. Salinity Laboratory, USDA-ARS, Riverside, CA.
USEPA. 2009. Final Effluent Guidelines. http://www.epa.gov/waterscience/guide/construction/ (Accessed on 7/17/2010).

USEPA. 2011. Status of Rulemaking to Revise Numeric Turbidity Limit. http://water.epa.gov/scitech/wastetech/guide/construction/index.cfm. (Accessed on 8/26/2011)

USEPA. 2002. National water inventory 2000 report. EPA-841-R-02-001. Office of Water, U.S. Environmental Protection Agency, Washington, DC.

Vacher, C. A., Loch, R. J., and Raine, S. R. (2003). Effect of polyacrylamide additions on infiltration and erosion of disturbed lands. Aust. J. Soil Res. 41, 1509–1520.

Wimbedy, J.W., and D.E. Jordan. 1971. An automated method for the determination of low concentrations of polyelectrolytes. Anal. Chim. Acta. 56:308-312.

Appendix 1. Abbreviations and symbols

CPM: Coastal Plain muck
CPS: Coastal Plain sand
DPAM: dissolved polyacrylamide
GPAM: granular polyacrylamide
HC: hydraulic conductivity
NTU: nephelometric turbidity units
PAM: polyacrylamide
PCL: Piedmont clay loam
PSL: Piedmont sandy loam
PV: pore volume
RSD: residual standard deviation
TOC: total organic carbon
TSS: total suspended solids

ΔH = head difference across the sample.
A = cross-sectional area of the soil sample
C = concentration of PAM in solution after the 24-h equilibration (mg L^{-1})
C/C_o = relative concentration
C_{im} = concentrations in immobile phases
C_m = concentrations in mobile phase
C_{md} = detection limit
D = dispersion coefficient
D_m = dispersion coefficient of mobile phase
k_d = distribution coefficient (L kg^{-1})
K_L = an affinity constant related to binding energy (L mg^{-1}).
L = characteristic length of the studied system (column length).
r^2 = coefficient of determination
R = retardation factor
S = amount of PAM adsorbed by soil (mg kg^{-1})
S_{max} = the Langmuir PAM sorption maxima (mg kg^{-1})
t = time
v = pore water velocity
v_m = average mobile pore water velocity
V_t = the total volume of soil (cm^3).
x = depth
y_{blank} = mean turbidity signal (NTU) of blank solutions containing hyamine but no PAM
α = chemical mass transfer coefficient between mobile and immobile liquid phases.
β = fraction of solute present in the mobile region under equilibrium conditions
θ_{im} = volumetric water content of mobile phase
θ_m = volumetric water content of immobile liquid phases
ρ_b = soil bulk density (g cm^{-3})
σ = standard deviation (n = 8) of turbidity in low PAM concentration samples
ω = ratio between hydrodynamic residence time and a characteristic time of solute movement in the immobile region

Appendix 2. Publications, presentations, efforts at technology transfer or communication of results to end users, policy makers, or others

Journal publications

1. Kang, J., T.D. Sowers, R.A. McLaughlin, O.W. Duckworth, A. Amoozegar, and J.L. Heitman. 2013. Turbidimetric determination of anionic polyacrylamide in low carbon soil extracts. Journal of Environmental Quality 42:1902-1907.
2. Kang, J., R.A. McLaughlin, J.L. Heitman, and A. Amoozegar. Erosion control blanket and polyacrylamide performance under rainfall simulation. Journal of Environmental Quality (*submitted*).
3. Kang, J., R.A. McLaughlin, O.W. Duckworth, J.L. Heitman, and A. Amoozegar. Transport of dissolved polyacrylamide in a sandy clay loam. Geoderma (*in preparation*).

Presentations

1. Tyler D. Sowers*, R.A. McLaughlin, M.Y. Andrews, J. Kang, and O.W. Duckworth. 2013. Developing field portable methods for polyacrylamide determination. Annual Meeting of the International Erosion Control Association. Feb 11-13, 2013, San Diego, CA.
2. Kang, J., T.D. Sowers, R.A. McLaughlin, O.W. Duckworth, J. Heitman, and A. Amoozegar, 2013. Optimizing environmental use of polyacrylamide for construction site runoff: PAM quantification. Annual Meeting of the Water Resource Research Institute of North Carolina. Mar 20-21, 2013, Raleigh, NC.
3. Kang, J., T.D. Sowers, R.A. McLaughlin, O.W. Duckworth, A. Amoozegar, and J.L. Heitman. 2013. Environmental use of polyacrylamide: detection in water. Joint US EPA & NCSU Interactive Collaboration Forum, Mar 28, 2013, RTP, NC.
4. Kang, J., R.A. McLaughlin, T.D. Sowers, O.W. Duckworth, J.L. Heitman, and A. Amoozegar, 2013. Quantification of aqueous polyacrylamide for soil and water conservation. 2nd Annual Postdoctoral Research Symposium of NC State University. June 5, 2013. Raleigh, NC.
5. Kang, J., and R.A. McLaughlin. 2014. Optimizing soil-polyacrylamide interactions for erosion control at construction sites. Annual Meeting of the Water Resource Research Institute of North Carolina. Mar 19-20, 2014, Raleigh, NC.

Technology transfer or communication of results to end users, policy makers, or others

The results are being communicated through publications in scientific journals and presentations at conferences and workshops, as indicated above. In addition, the information will be incorporated to ongoing training through the PI's Extension program, local and regional workshops for contractors and agencies, and trade and association newsletters.